4-2016

Differentiating Saginaw from Huron-Erie Ice Lobe Meltwater Deposits in South Central Michigan Using Longitudinal Profiles, Grain Size Analysis, and Lithology

Nathan R. Erber

DIFFERENTIATING SAGINAW FROM HURON-ERIE ICE LOBE MELTWATER DEPOSITS IN SOUTH CENTRAL MICHIGAN USING LONGITUDINAL PROFILES, GRAIN SIZE ANALYSIS, AND LITHOLOGY

by

Nathan R. Erber

A thesis submitted to the Graduate College
in partial fulfillment of the requirements
for the degree of Master of Science
Geosciences
Western Michigan University
April 2016

Thesis Committee:

Alan E. Kehew, Ph.D., Advisor
Robb Gillespie, Ph.D.
Duane R. Hampton, Ph.D.

DIFFERENTIATING SAGINAW FROM HURON-ERIE ICE LOBE MELTWATER DEPOSITS IN SOUTH CENTRAL MICHIGAN USING LONGITUDINAL PROFILES, GRAIN SIZE ANALYSIS, AND LITHOLOGY

Nathan R. Erber, M.S.

Western Michigan University, 2016

The Saginaw and Huron-Erie lobes of the Laurentide Ice Sheet had a significant impact on the landscape of south-central Michigan after the Late Glacial Maximum. During the advances and retreats of these lobes, a complicated network of meltwater channels developed. Two goals of this study are: 1) to use sand-grain lithology, grain-size analysis, and longitudinal profiles to determine if a difference exists between Saginaw lobe and Huron-Erie lobe meltwater deposits; and 2) to determine if a large meltwater sluiceway containing the modern St. Joseph River had a source of meltwater and outwash from the Huron-Erie lobe. Two cores from drumlinized uplands formed by the Saginaw lobe were compared to three cores from the St. Joseph sluiceway that, based on longitudinal profiles, carried meltwater from the Huron-Erie lobe. Grain-size and sand-grain lithology analysis were conducted on these five cores. The sand-grain lithology analysis indicates a significant difference in shale content between the cores within the channelized lowland and the drumlinized uplands. Increased shale content within the channelized lowlands is likely derived from Paleozoic shales within the flow path of the Huron-Erie lobe (Coldwater, Antrim, Sunbury, Bedford Shales). Longitudinal profiles and mapping of the channelized lowlands show a gentle gradient from east to west indicating a meltwater source from the Huron-Erie lobe.

ACKNOWLEDGMENTS

I would like to thank Dr. Alan Kehew for all of his guidance and advice in helping me through the process of my thesis project. I would also like to thank my thesis committee, Dr Robb Gillespie for his support and assistance of me in developing ideas for this project, and Dr. Duane Hampton for his collaboration and advice. The faculty and students of the WMU Department of Geosciences also deserves thanks for all of their help in preparing me to reach the culmination of this project. I thank the faculty for their instruction in the classroom and am grateful to fellow students, for their friendly support.

I would also like to express my gratitude toward my family. I cannot express enough how grateful I am for my wife, Andrea, for being patient, loving, and understanding as I spent long hours commuting, working, and counting sand grains. I would also like to thank my parents for their support throughout my life and leading me toward successfully achieving my goals.

Nathan R. Erber

TABLE OF CONTENTS

Table of Contents–Continued

CHAPTER

Table of Contents−Continued

CHAPTER

LIST OF TABLES

LIST OF FIGURES

List of Figures−Continued

CHAPTER I

INTRODUCTION

Sub-lobes of the Laurentide Ice Sheet significantly influenced south-central Michigan immediately after the Late Glacial Maximum (LGM). These sub-lobes are classified as the: (1) Lake Michigan lobe, (2) Saginaw lobe, and (3) Huron-Erie lobe. During the many advances and retreats, a complicated network of meltwater channels developed. This network of channels has been investigated at a regional scale. One major focus of this study is to compare the lithology of outwash sediments deposited within a specific meltwater channel with those deposited outside the channel to identify the provenance of the outwash. Two specific goals of this study are to: 1) use sand grain lithology, grain size analysis, and longitudinal profiles to determine if a difference exists between Saginaw lobe and Huron-Erie lobe meltwater deposits; and 2) determine if a large meltwater sluiceway containing the modern St. Joseph River had a source of meltwater and outwash from the Huron-Erie lobe. Successful use of sand grain lithology to determine the source of outwash deposits will aid in future mapping and understanding of ice lobe interactions in southern Michigan.

Study Area

The study area is located in Branch, Calhoun, Jackson, and Hillsdale counties in south-central Michigan (Figure 1). A large east-west trending meltwater channel, which is referred to as the St. Joseph sluiceway, is the focus of this study. Two modern-day rivers flow in the St. Joseph sluiceway, including the south branch of the Kalamazoo River and the main branch of the St. Joseph River. Between 2014 and 2015, one rotosonic and four geoprobe borings were drilled

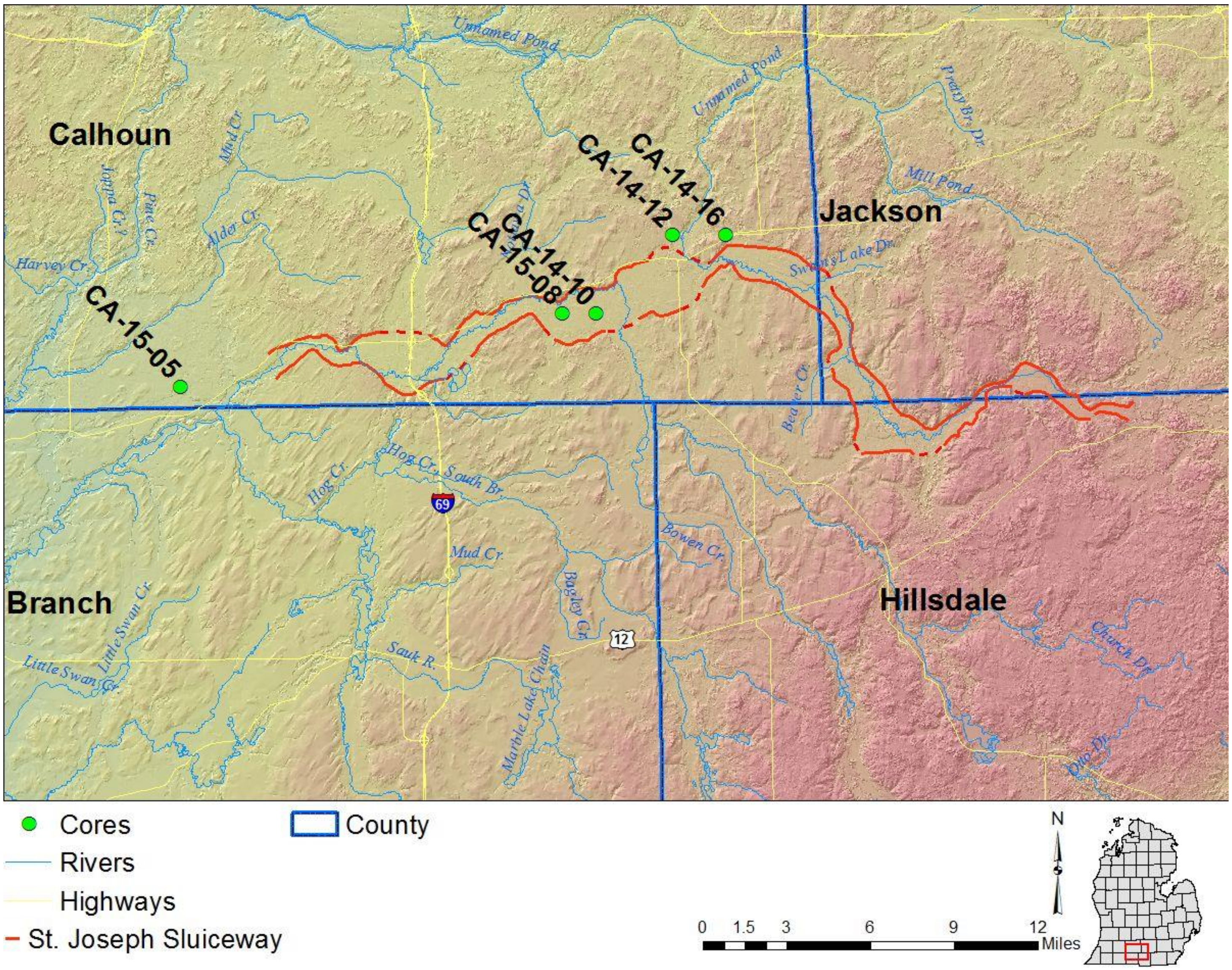

Figure 1. Study area and borehole locations.

in a portion of the study area, primarily in Calhoun County and immediately adjacent areas. These borings were selected to represent deposits both inside and outside the St. Joseph sluiceway.

Cores within this study are divided into two groups to test the hypothesis that deposits of the drumlinized uplands are derived from the Saginaw lobe, and that deposits within the St. Joseph sluiceway are derived from the Huron-Erie lobe. The first group of boreholes (CA-14-10, CA-15-05, and CA-15-08) are located in the St. Joseph sluiceway. The second groups of boreholes (CA-14-12 and CA-14-10) are located on the drumlinized uplands adjacent to the St. Joseph sluiceway. These borehole locations were specifically selected either within the St. Joseph sluiceway or on the adjacent uplands to determine the relationship between the two landforms.

Previous Investigations

Leverett and Taylor (1915) were the first to map the glacial deposits of Michigan basin their work on glacial landforms. They were the first to associate end moraines with ice marginal positions for the Saginaw and Huron-Erie lobes. Martin's (1955) revised map of glacial deposits in Michigan delineated the distribution of glacial landforms of Michigan's Lower Peninsula. Farrand and Bell (1982) published a Quaternary geology map of the state which included textural descriptions based on previous soil surveys completed in Michigan. Monaghan and Larson (1986) correlated two till units (Bedford and Fulton tills) of the Saginaw lobe by using grain size distribution and clay mineralogy of the tills. Monaghan and Larson (1986), with their study, were able to link the (1) Kalamazoo moraine of the Saginaw lobe, to the (2) Kalamazoo moraine of the Lake Michigan lobe, and the (3) Powell moraine of the Huron-Erie lobe. More recent research has focused on the surface morphology and the influence of both subglacial and

proglacial meltwater in the Saginaw lobe terrain (Taylor et al., 1998; Fisher and Taylor, 1999; Kozlowski, 1999; Kehew et al., 1999; Kozlowski et al., 2001; Fisher et al., 2003, 2005; Kozlowski et al., 2004; Kozlowski et al. 2005; Kehew et al 2012a). Kehew et al. (2012a) described four landsystems to better classify the Saginaw lobe surface terrain. The landsystems approach of classification was based, in part, on a proposed relationship between ice dynamics and bedrock lithology of the Saginaw lobe. Kehew et al. (2012b) were also able to relate ice sheet dynamics to the importance of subglacial meltwater and the formation of tunnel valleys. The Saginaw and Huron-Erie lobes have been suggested as possible sources of meltwater for large meltwater flooding events (Curry et al., 2014). Curry et al. (2014) suggested that the source water for the Kankakee torrent might have been derived from the Lake Michigan, Saginaw, and Huron-Erie lobes of Michigan and northern Indiana. They also advance the asynchronous relationship between the three Michigan lobes and point to the Huron-Erie lobe as being the last active lobe in the region.

Saginaw and Huron lobe ice flow paths both originate in the Canadian Shield northeast of Georgian Bay and the Niagara Escarpment. Moving toward the southeast, they then combine to form the Saginaw-Huron Ice Stream (Eyles, 2012). South of the Niagara Escarpment, the Saginaw-Huron Ice Stream became more lobate and separated into distinct flow paths. The general flow direction of the Saginaw lobe was southwesterly from Saginaw Bay. The Huron and Erie lobes had different sources during the Late Wisconsin. The Erie lobe was a separate lobe emanating from the Grenville Province in the Canadian Shield (Howard et al., 2012). Separate Late Wisconsin Huron and Erie lobes flowing in the Lake Huron and Lake Erie basins, respectively, converged to form the Huron-Erie lobe (Howard et al., 2012). The merged Huron-Erie lobe flowed into the study area in a west/southwestward direction.

Bedrock underlying the Saginaw lobe flow path consists mostly of Paleozoic rocks (downstream Michigan Basin portion of the flow path) and Precambrian crystalline rocks (Canadian Shield near the head of the ice stream Eyles, 2012). Specific Paleozoic rocks underlying the Saginaw lobe are the Coldwater Formation, Marshall Formation, Michigan Formation, Saginaw Formation, Grand River Formation, Bayport Limestone, and Ionia Formation. Bedrock underlying the Huron-Erie lobe flow path consisted mostly of Paleozoic rock (Marshall Formation, Coldwater Formation, Sunbury Shale, Berea Sandstone, Bedford Shale, Antrim Shale, Traverse Group, Dundee Limestone, Detroit River Group, Sylvania Sandstone, Bass Island Group, Salina Group, and Garden Island Formation). Canadian Shield rocks were also present under the Huron-Erie lobe near the source of the Saginaw-Huron Ice Stream and the Erie lobe.

Studies conducted to differentiate lobe deposits of the Laurentide Ice Sheet in the Midwest using lithology of glacial grains include Anderson (1957), Shah (1971), Lovan (1977), and Hobbs (1998). Anderson (1957) used clast counts from tills to differentiate glacial lobes in Michigan, showing that provenance was a mixture of Canadian Shield crystalline rocks and Paleozoic sedimentary rocks of the Michigan basin. Results of this study indicated that the Saginaw lobe was the only lobe that had a unique lithology (Lorrain Quartzite). Anderson (1957) showed that using relative proportions of lithology are the best way to differentiate glacial lobes. The conclusions of Anderson (1957), with regard to the sand fraction counts, determined that counts alone revealed little about the source of a till; however, because the sand lithology was consistent throughout the lobe, such counts are valuable in differentiating between deposits of the same lobe.

Shah (1971) attempted to map the lithologic distribution of glacial deposits in southwest Michigan as part of an economic glacial aggregate evaluation. This study produced isopleth maps for Precambrian lithologies and Paleozoic lithologies within Kalamazoo County. Results indicated significant differences are apparent between the Lake Michigan lobe and Saginaw lobe deposits, and lithologic proportions are important in differentiating between the two. Precambrian content (metamorphic and igneous clasts) were higher in Saginaw lobe deposits than in Lake Michigan lobe deposits. Paleozoic lithology had a high variability in the Kalamazoo County study area, which Shah (1971) attributed to local erosion and plucking. Based on the distribution of the lithologic categories Shah (1971) determined that carbonate and chert percentages were higher in Lake Michigan lobe deposits compared to Saginaw lobe deposits. No other distinct isopleth patterns emerged based solely on Paleozoic lithologic clast counts.

Lovan (1977) used textural and mineralogical analysis of selected tills in southwest Michigan to define an interlobate boundary between the Lake Michigan lobe and the Saginaw lobe by the use of heavy mineral ratios and X-ray diffraction of clays.

Hobbs (1998) demonstrated the use of the 1-2mm size sand fraction to determine provenance and to differentiate between glacial till deposits in Minnesota. Hobbs (1998) outlined the methods and significance that sand-grain lithology studies have in differentiating between glacial lobes, concluding that using sand-grain lithology is a useful tool in differentiating between various glacial lobe deposits.

Determining flow paths and sediment provenance is helpful both in characterizing individual lobe sediment lithology and in differentiating lobes. The distribution of Paleozoic bedrock of Michigan is shown in Figure 2. Shale-rich bedrock is present along the flow path of

the Huron-Erie lobe; and therefore, deposits from this ice lobe should contain a higher percentage of shale grains than Saginaw lobe deposits. Shale formations that the Huron-Erie lobe overrode include the Bedford, Antrim, Sunbury, and Coldwater Shales. Shale bedrock is less abundant under the Saginaw ice lobe flow path; therefore, Saginaw lobe deposits should have lower shale content. The Saginaw Formation, Michigan Formation, Marshall Formation, and Coldwater Formation are the significant Paleozoic bedrock units underlying the Saginaw lobe. These rock units, with the exception of the Coldwater Shale, are composed of sandstone, limestone, dolomite, and evaporates. Sediments deposited during the late Wisconsin were a combination of recycled material from previous advances and retreats and new actively eroded bedrock incorporated into the glacial deposits.

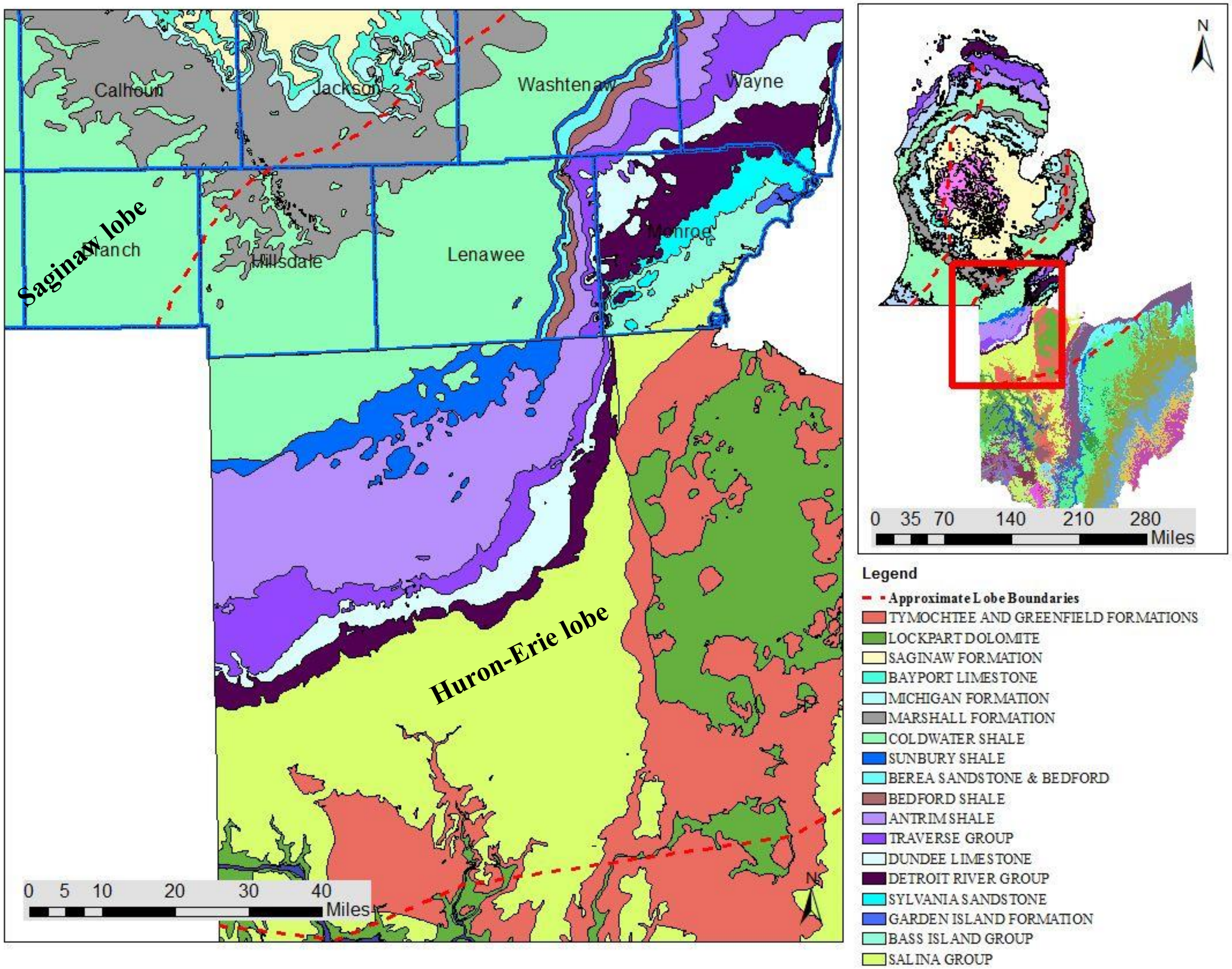

Figure 2. Regional bedrock geology of Michigan and Ohio (Bedrock Geology of Michigan, 1987; Ohio Division of Geological Survey, 2006).

CHAPTER II

GEOLOGY

Bedrock Geology

Glacial deposits in south-central Michigan are composed of both eroded local and far traveled bedrock that the Laurentide Ice Sheet overrode during its advances. Bedrock formations overridden by the ice sheet are important to understanding glacial flow paths and differentiating between glacial lobes. The eroded surface of the Michigan basin consists of Paleozoic sedimentary rocks (mainly sandstone, shale, carbonates, and evaporates) that occur in concave upward beds (refer to Figures 2). Topography and bedrock lithology exerted an important primary control on Laurentide Ice Sheet lobe movement. Bedrock permeability and porosity not only influenced pore water pressure at the ice base, but ultimately, also the subglacial hydrology and basal shear stress of the ice flow (Kehew et al., 2012a).

The Michigan basin is an intracratonic basin that was infilled during late Precambrian through Pennsylvanian time. It is bounded to the north and east by the Canadian Shield, the south by the Findlay Arch and the west by the Wisconsin Arch (LoDuca, 2009). The basin consists of sedimentary rocks mostly deposited in shallow marine conditions during the Paleozoic Era. The Canadian Shield underlying and immediately surrounding the Michigan basin consists of Precambrian plutonic and volcanic igneous rocks, and high-grade metamorphic rocks (Gillespie et al., 2008).

Bedrock formations that subcrop within the study area include the Coldwater Shale and the Marshall Sandstone (Figure 3).

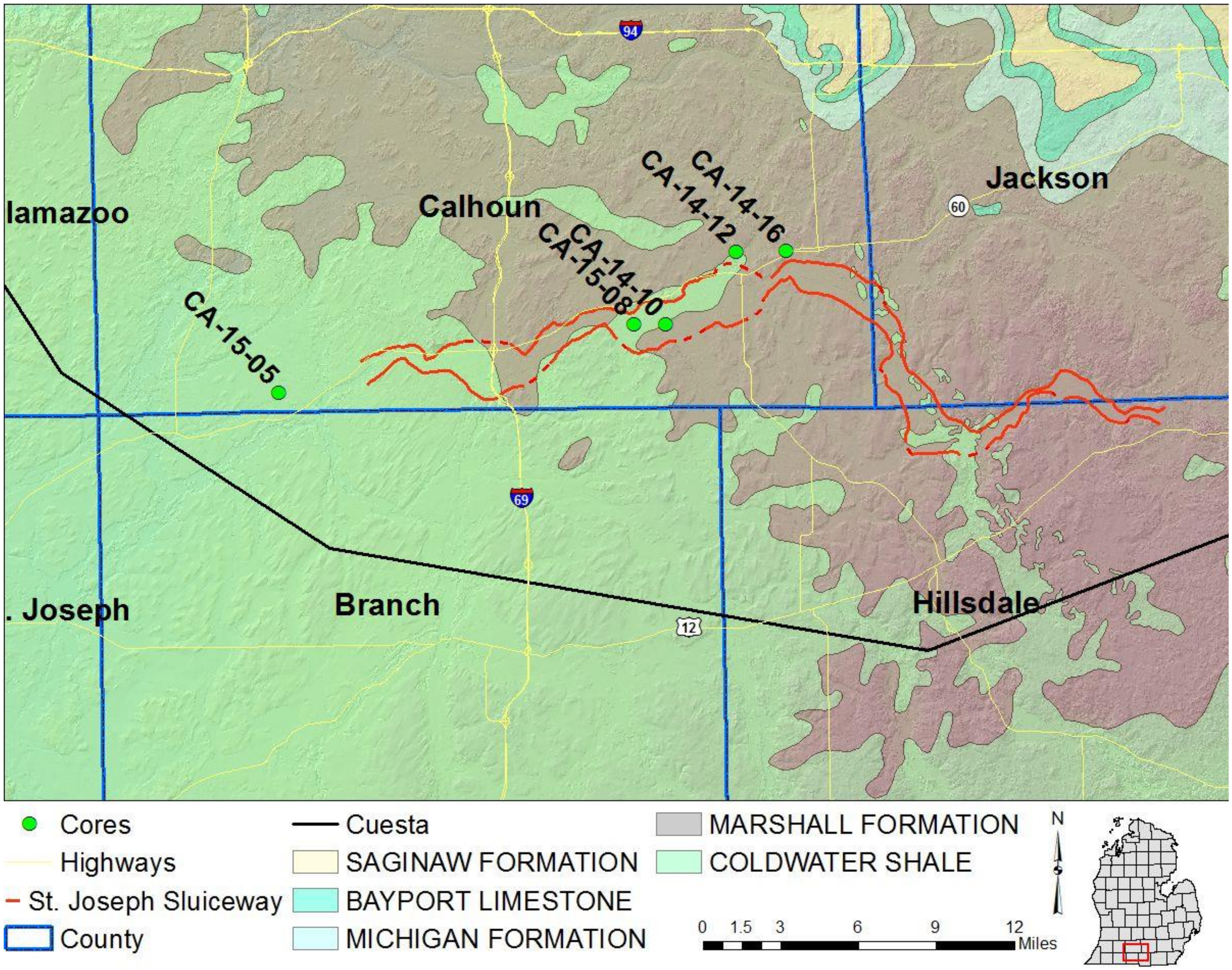

Figure 3. Detailed bedrock geology of study area (Bedrock Geology of Michigan, 1987).

Mississippian Coldwater Shale consists of gray to bluish-gray shale with thin interbeds of limestone, dolomite, siltstone, and sandstone (Dorr and Eschman, 1970; LoDuca, 2009). The fine-grained sediments of this formation were deposited in an offshore marine environment (Dorr and Eschman, 1970; LoDuca, 2009). The Coldwater Shale crops out in the Coldwater River valley near the town of Coldwater and elsewhere in Branch and Hillsdale Counties. Outcrops also occur along Lake Huron in Huron and Sanilac Counties. Coldwater Shale subcrops within the study area in southern Michigan and northern Indiana.

The Mississippian Marshall Sandstone consists of gray, green, pink and red sandstones and siltstones. The Marshall Sandstone was deposited in a nearshore and beach environment, which covered the Michigan Basin during middle Mississipian time (Dorr and Eschman, 1970; LoDuca, 2009). Marshall Sandstone subcrops in the northeastern portion of the study area. There is a buried bedrock cuesta which roughly follows the Marshall Sandstone and Coldwater Shale contact (refer to Figure 3). The northeastern portion of the cuesta is formed by the Marshall Formation; whereas, the southeastern is formed by the Coldwater Shale (Rieck and Winters, 1982). The Saginaw and Huron-Erie lobe boundary is a result of this Marshall Sandstone and Coldwater Shale cuesta (Rieck and Winters, 1982). The cuesta acted as a barrier to the Huron-Erie lobe, ultimately limiting its encroachment toward the northwest into Saginaw lobe terrain.

Wisconsin Glaciation

Time-transgressive diachronic units are used for glacial drift deposits. Such deposits have time-parallel boundaries that do not correlate across large areas (Larson and Kincare, 2009). This is typical of till deposits that vary in age from proximal to distal locations. Diachronic units based on event classification were proposed by Johnson et al. (1997) and are

used in this study. The most recent glacial event to occur in south-central Michigan was the Wisconsin Episode. The episode is divided into three subepisodes, Ontario (Early), Elgin (mid), and Michigan (late) (Johnson et al., 1997; Karrow et al., 2000; Larson and Kincare, 2009). The majority of surficial glacial drift deposits in Michigan were deposited during or after the Michigan subepisode, which in turn, was after the Late Glacial Maximum approximately 23,000 cal yr BP (Curry and Petras, 2011). Three distinct lobes developed through the Michigan region after the Late Glacial Maximum. These are the: (1) Saginaw lobe, (2) Huron-Erie lobe, and (3) Lake Michigan lobe. (1) Saginaw lobe ice in Michigan advanced from Saginaw Bay southwestward toward the study area. (2) The Huron-Erie lobe covered the Lake Huron and Lake Erie basins and extended southwestward into Michigan. (3) Lake Michigan lobe ice covered the Lake Michigan Basin and extended eastward and southeastward into western Michigan. The Saginaw lobe was first to retreat after the Late Glacial Maximum (Figure 4). Thereafter, advances and retreats of the three lobes were asynchronous (Kehew et al., 2005; Curry et al., 2014).

Saginaw Lobe Landsystems

Kehew et al. (2012a) describe four landsystems within the Saginaw lobe terrain (Figure 5). Cores CA-14-12, CA-14-16, CA-14-10, CA-15-08 and CA-15-05 are all located within Landsystem 1. Landsystem 1, the most distal of the landsystems to the southwest, encompasses the Sturgis Moraine and a drumlinized till plain to the northeast, the Union Streamlined Plain (Dodson, 1985). The Sturgis Moraine, a terminal/recessional moraine, displays about 25m of relief, and consists mostly of glaciofluvial sediments with thick alluvial fans sloping southward off the distal slopes of the moraine. Buried, early stage, subglacial, tunnel valleys are oriented across the moraine in a northeast-southwest direction (Nicks, 2004). Drumlinized till plains

capped by sandy diamicton, overlie Coldwater Shale and Marshall Sandstone to the north of the moraine. These drumlins are located on upland tracts adjacent to channel-like lowlands. Kehew et al. (2012a) proposed that the impermeable underlying Coldwater Shale caused high basal pore water pressure, which in turn caused deformation of basal sediments into drumlins. Fisher and Taylor (2002) and Fisher et al., (2003; 2005), suggest an alternative hypothesis in which drumlins on the uplands were formed by an erosional subglacial sheetflow.

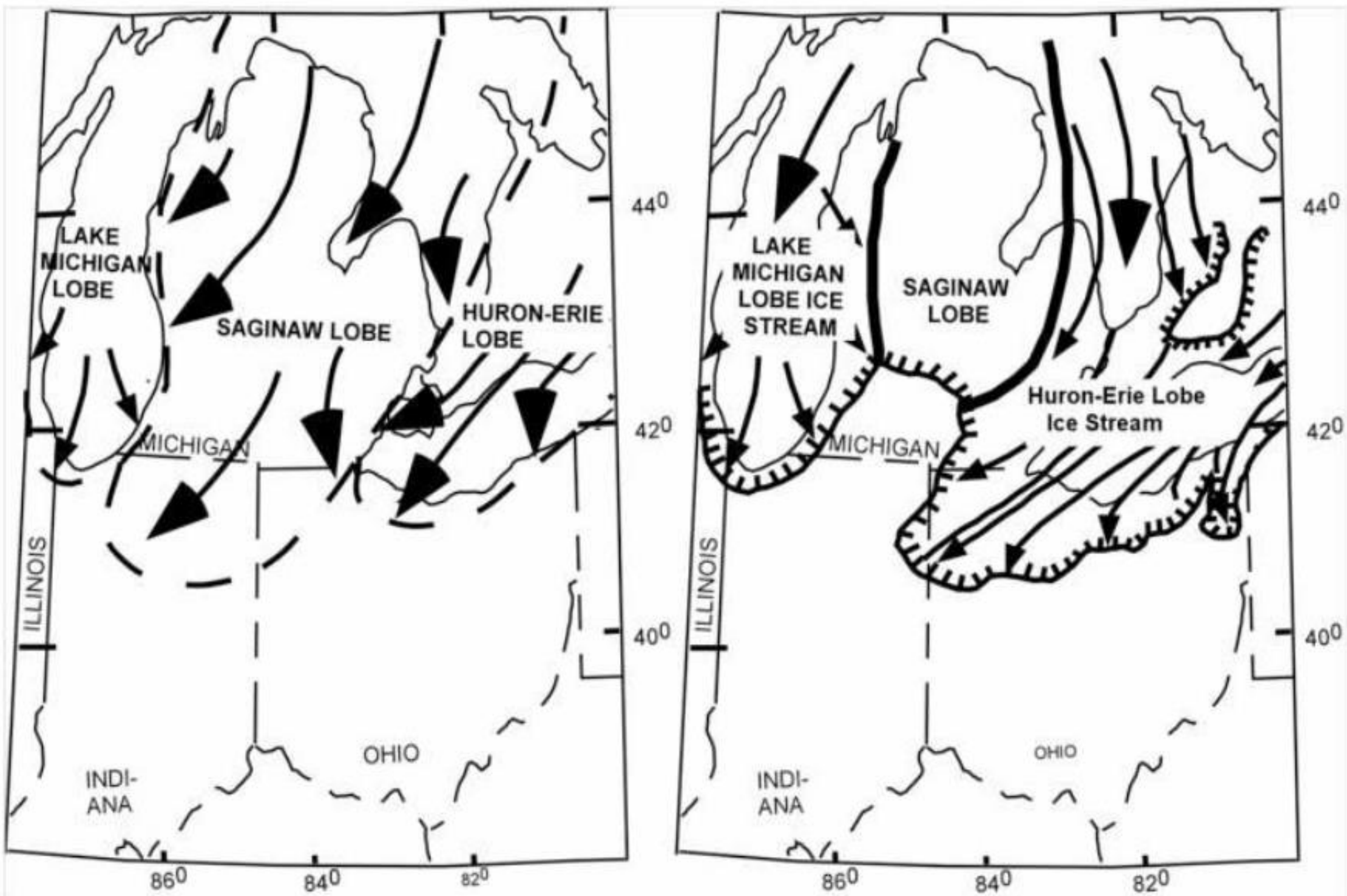

Figure 4. Relative locations of the Saginaw, Huron-Erie, and Lake Michigan lobes (Kehew et al., 2005). Left figure shows re-advance of the Saginaw lobe after LGM approximately 21 BP. Right figure shows retreat of the Saginaw lobe approximately 15 – 16 BP.

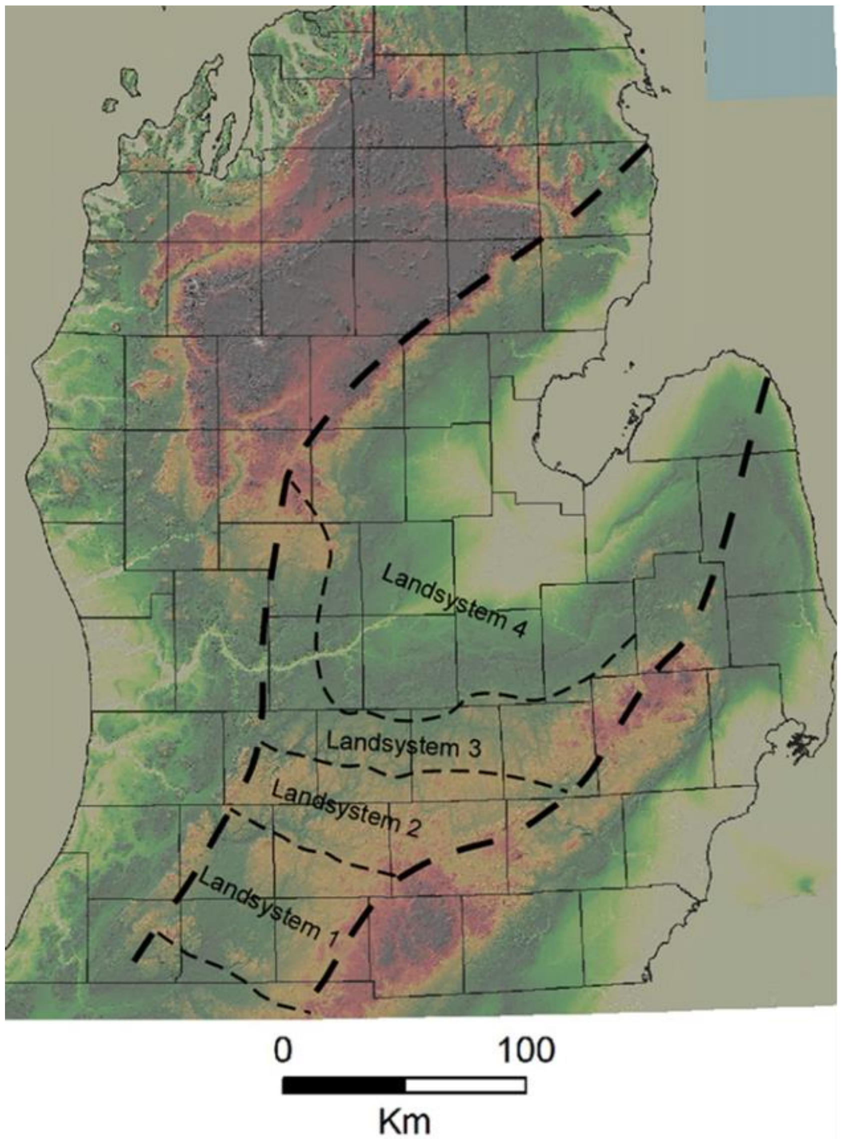

Figure 5. Geographic extent of Saginaw lobe Landsystems (Kehew et al., 2012a).

CHAPTER III

METHODS

Data in this study come from five borings collected in Calhoun County. The borings were drilled as part of "The Michigan Geological Survey" mapping projects funded by the "US Geological Survey STATEMAP" and "Great Lakes Geologic Mapping Coalition" programs. Cores were taken to the Soil Laboratory at Western Michigan University for grain size and sand grain lithology analysis. The following procedures were used.

Grain Size Analysis

Sieving methods for this study were modified from Ewald (2012). Similar methods have also been employed by Bowles (1978), Flint (1999), Barnes (2007), Beukema (2003), and Woolever (2008). Two sieving techniques were used to separate the sieve fractions: (1) a dry method for coarse samples, and (2) a wet method for finer samples. Initial sample weight was consistently between 400-500 grams, depending on the water content of the sample.

Dry-Coarse sample procedure:

- One 400-500 gram sample was taken from the core and placed in an aluminum pan to dry for 24 hours in an oven.
- The sample, once dry, was gently disaggregated with a mortar pestle and the weight was recorded.
- The disaggregated sample was placed in a sieve stack of seven sieves in order from top to bottom: #5, #10, #18, #35, #60, #120, #230, and bottom pan. The sieve stack was then placed in a RoTap machine (Figure 6) and shaken for ten minutes.

- Once shaken, the contents of each sieve were individually removed, weighed, recorded, and placed in a plastic bag.
- Bottom pan contents were removed, weighed, and placed in a separate plastic bag.
- The weight of each sieve was used to calculate a normalized weight percent for each sieve fraction.

Wet-Fine sample procedure:

- One 400-500 gram sample was taken from the core and placed in an aluminum pan to dry for 24 hours in an oven.
- Once dry, the sample was gently disaggregated with a mortar and pestle and the weight was recorded.
- The disaggregated sample was placed in a large cup and topped off with water.
- Contents of the cup were then stirred for one minute and washed through a #230 sieve with pan underneath.
- Contents of the #230 sieve were washed into an aluminum pan and placed in the oven to dry for later dry sieving procedure.
- Contents of bottom pan were also put into an aluminum pan in the oven to dry, and then stored in a plastic bag.
- The weight of each the #230 sieve and bottom pan were then used in the dry sieving and clay/silt separation procedures to calculate a normalized weight percent.

Figure 6. Grain size analysis tools. Sieve stack inside the RoTap machine.

The clay and silt separation procedure:

- About 10 grams of the bottom pan sample (from both the dry and wet sieving procedures) was collected and placed into a 1000 ml beaker. If the entire sample was less than 10 grams, the whole sample was used.
- The sample was then dispersed using an alkaline solution of 0.5% sodium hexametaphosphate ($Na_6O_{18}P_6$) which was poured over the 10 gram sample to act as a deflocculant. The beaker was filled to 700ml with the solution.
- The sample was then agitated for 10 seconds and placed into an ultrasonic vibration bath for 20 minutes.
- The sample was then allowed to settle for two hours. During this time frame, the clay would stay in suspension and the silt would settle to the bottom of the beaker.
- The suspended clay and settled silt were then poured into separate pre weighed aluminum pans. The individual pans were then placed into an oven to dry for 24 hours.
- Once dry, the weight of the sample and pan was then recorded and incorporated into the normalized weight percent calculations for the core.

Lithology

Procedures to determine sand grain composition (as used in this study) were modified from Hobbs (1998). Similar methods have been used by Anderson (1957) and Shah (1971). Sand grain lithology can be easily incorporated into a textural analysis of sediment samples. Sand counting and lithologic identification was conducted for 6-9 samples from each core in the study area. Samples were collected based on depth in the core.

Figure 7. Sieve fractions used for lithology methods.

Table 1
Sand Grain Lithology Data Collection Chart

Sample: CA-14-12 (0-5)

Lithology	**Sieve #10**		**Sieve #18**	
	Number	**Percentage**	**Number**	**Percentage**
Shale	8	8	8	8
Mafic	19	19	12	12
Felsic	26	26	30	29
Quartzite	29	29	15	15
Quartz Grain	13	13	30	29
Clastic	5	5	7	7
Limestone/Dolomite	0	0	0	0
Total	**100**	**100**	**102**	**100**

Two to three samples were taken from the top, middle, and bottom of each core (a total of 6-9 samples) in order to represent vertical intervals. This allowed an overall analysis of the core without having to analyze every inch of the core. Sand grain lithology was determined for sieve fractions #10 (2-4mm) and #18 (1-2mm) (Figure 7). Samples of at least 100 grains were placed in small Petri dishes for counting under a binocular microscope. After one hundred grains were counted, this fraction was separated for further analysis. This group was then divided based on lithology, and the various lithology groups were counted (Table 1).

The lithology groupings used in this study is a simplified version of one used by Hobbs (1998). The classification system uses seven basic groupings (shale, mafic, felsic, quartzite, quartz grain, clastic, and limestone/dolomite). These groups were either a stand-alone lithologic grouping or a combination of several lithologic types. Grouping rock types was necessary because the small size of the grains did not allow ready and reliable differentiation between some rock types.

Shale Group

The shale group includes shale fragments varying in color from black to grey, and are soft and very easy to scratch with forceps. Despite the variations of color, shale grains were defined as a single grouping to determine if shale lithology specifically could be used to differentiate between Saginaw and Huron-Erie lobe deposits.

Mafic Group

The mafic grouping contains both dark colored igneous and metamorphic grains. Grouping these two lithologies together is largely done because of the difficulty in clearly differentiating between them in the 1mm-2mm size fraction.

Felsic Group

Felsic group grains consisted of light-colored igneous lithologies. Grains in this grouping resemble small felsic crystalline clasts. They are largely composed of quartz in conjunction with other minor minerals such as biotite, amphibole, and pyroxenes.

Quartzite Group

The quartzite group is a combination of light colored quartzite and chert grains. The Lorrain Formation (Jasper Conglomerate) had previously been established as an indicator for Saginaw lobe deposits (Leverett and Taylor, 1915; Anderson, 1957; Howard et al., 2012). Bulding on this previous work, the quartzite group was formed to aid in differentiating between Saginaw and Huron-Erie lobe deposits within this study area.

Quartz Grain Group

The Quartz Group consisted of pure quartz grains with no identifiable other minerals. The fragments are classified in the felsic group if there are other trace minerals in the grain.

Clastic Group

This group consisted of clastic sedimentary rock fragments (ie sandstone and other fine-grained clastic grains). These clasts tended to be fissile and loosely consolidated. Shale grains are not included in this group.

Limestone/Dolomite Group

All rock fragments that effervesce readily in dilute HCL are counted in the Limestone/Dolomite Group.

Once grains are separated by lithology, the number of each category is determined, and then these counts are converted into percentages.

Longitudinal Profiles and Map

ArcGIS is used to display delineated meltwater channels associated with the Saginaw and Huron-Erie lobes. Data based on longitudinal profiles, Digital Elevation Models (DEMs), Quaternary and bedrock geologic maps are all integrated in this study. These data were used in ArcGIS to create maps and profiles to aid in determining the difference between the cores located in the drumlinized upland areas and cores located in the St. Joseph sluiceway.

DEMs are used in the initial mapping of the study area. Scarps are visible along the St. Joseph sluiceway and are used to define the boundaries and extent of the sluiceway. Identifiable terrace deposits are also apparent and mapped within the defined boundary of the sluiceway. Several profiles are also made within the St. Joseph sluiceway. Also, a longitudinal profile from the eastern to the western extent of the sluiceway was created. Elevations of selected points along existing rivers in the meltwater channel were extracted and compiles into the profile. Terrace deposit profiles were also created by choosing single points to represent each terrace deposit and extracting an elevation from that point. Broader scale-features, such as scarps, were mapped and profiles constructed to better understand the origin and subsequent history of the meltwater channels in the study area.

CHAPTER IV

RESULTS

Five borings from which cores were collected were drilled in Calhoun County, south-central Michigan. Two borings are located in the drumlinized upland and three are located in the channelized lowlands, all within Landsystem 1. The following core results are catagorized based on the landform in which they were drilled. Each core is described using a sand-grain lithology classification system modified from Hobbs (1998). Besides core descriptions, several longitudinal profiles and two complete textural analyses (cores CA-14-10 and CA-14-16) are presented.

Drumlinized Upland: Outside of St. Joseph Sluiceway

Core CA-14-12

Core CA-14-12 is located in the drumlinized upland just north of the St. Joseph sluiceway (Figure 8). Besides being located in the drumlinized upland, the boring is also located in an outwash fan at the end of a tunnel valley. Stratigraphy of the core consists of light tan to brown sand and gravel. The total depth of the core is 55 feet. Bedrock underlying this core is the Marshall Formation, consisting mostly of sandstone. No complete textural analysis is done for this core.

Lithology results for the core are shown in Table 2. This core, on average, has high percentages of limestone/dolomite and felsic material. Shale is the lowest percentage material in the core. Table 2 indicates that there is a difference between the size fractions of the 1-2 mm (#18) and 2-4 mm (#10) grains. Overall, mafic, quartzite, clastic, and limestone/dolomite groupings have a higher percentage of the 2-4 mm size fraction.

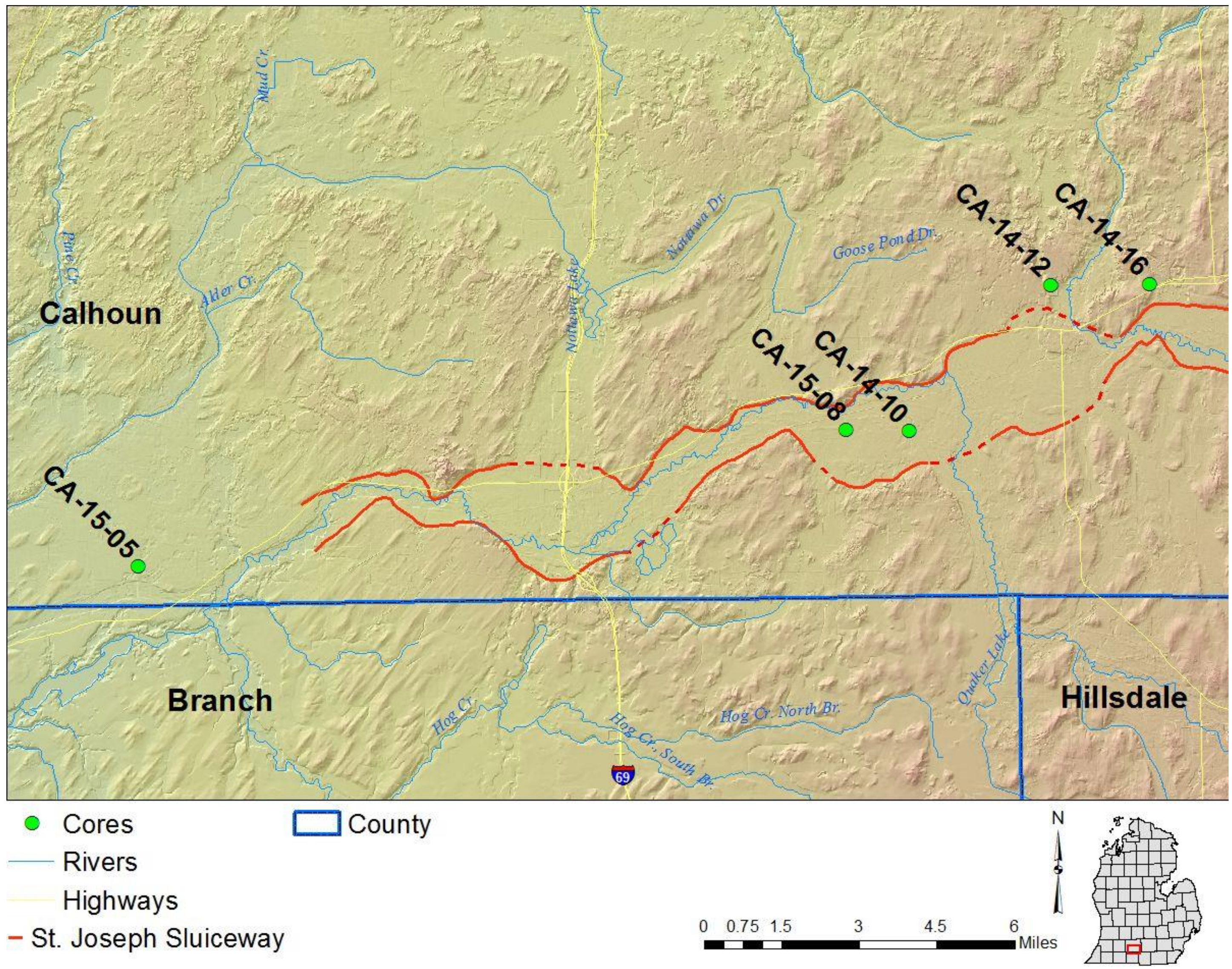

Figure 8. Locations of all five cores used in the study. Note: Cores CA-14-12 and CA-14-16 are located in drumlinized upland areas. Cores CA-14-10, CA-15-05, and CA-15-08 are located in the channelized lowlands.

Table 2

Core CA-14-12 Lithology Results (%)

Lithology	Shale		Mafic		Felsic		Quartzite		Quartz Grain		Clastic		Limestone / Dolomite	
Sample	**Sieve #10**	**Sieve #18**	**Sieve #10**	**Sieve #18**	**Sieve #10**	**Sieve #18**	**Sieve #10**	**Sieve #18**	**Sieve #10**	**Sieve #18**	**Sieve #10**	**Sieve #18**	**Sieve #10**	**Sieve #18**
0-5	8	8	19	12	26	29	29	15	13	29	5	7	0	0
5-10	3	0	5	6	17	29	19	17	8	19	17	7	31	21
10-15	2	0	9	3	25	28	31	17	5	28	4	3	24	20
20-25	2	2	16	3	17	27	19	17	7	21	10	9	29	21
25-30	3	1	11	13	18	22	15	10	6	22	11	10	36	22
40-45	3	4	6	5	24	28	29	22	9	23	6	5	24	13
45-50	2	4	5	9	24	11	32	18	9	25	8	5	20	28
50-55	1	2	6	5	22	23	36	14	11	28	8	10	16	18
Average	3	3	10	7	22	25	26	16	8	24	9	7	23	18

Note: Numbers represent percentages of a specified lithology for each sample. Light grey lines separate upper, middle, and lower sample groupings in the core.

Quartz grain and felsic lithologies have a higher percentage in the 1-2 mm size fraction. Shale lithology displays an identical percentage between the two size fractions.

Core CA-14-16

Core CA-14-16 is located in the drumlinized uplands just north of the St. Joseph sluiceway (refer to Figure 8). Stratigraphy of the core consists of an upper and lower diamicton with a middle silt/clay interval. Total depth of the core is 138 feet. Bedrock underlying this core is the Marshall Formation, which consists mostly of sandstone. Complete textural analysis was completed for this core (Figure 9). The upper diamicton displays an average normalized texture of 67.69% sand, 26.72% silt, and 5.59% clay. The middle section of silt and clay displays an average normalized texture of 8.71% sand, 45.90% silt, and 45.39% clay. The lower diamicton displays an average normalized texture of 60.83% sand, 32.08% silt, and 7.09% clay.

Lithology results for the core are shown in Table 3. This core, on average, has high percentages of limestone/dolomite and felsic material. Shale and mafic material make up the lowest percentages in this core.

Table 3 indicates that there is a difference between the size fractions of 1-2 mm (#18) and 2-4 mm (#10) grains. Overall, mafic, quartzite, clastic, and limestone/dolomite groupings have a higher percentage in the 2-4 mm (#10) size fraction. Quartz grain and felsic grains have a higher percentage in the 1-2 mm (#18) size fraction. Shale lithology displays an identical percentage in both size fractions. Higher amounts of clastic material are displayed in the lower diamicton unit. The difference between the two diamicton units suggests that more bedrock was being actively eroded and incorporated into the lower diamicton.

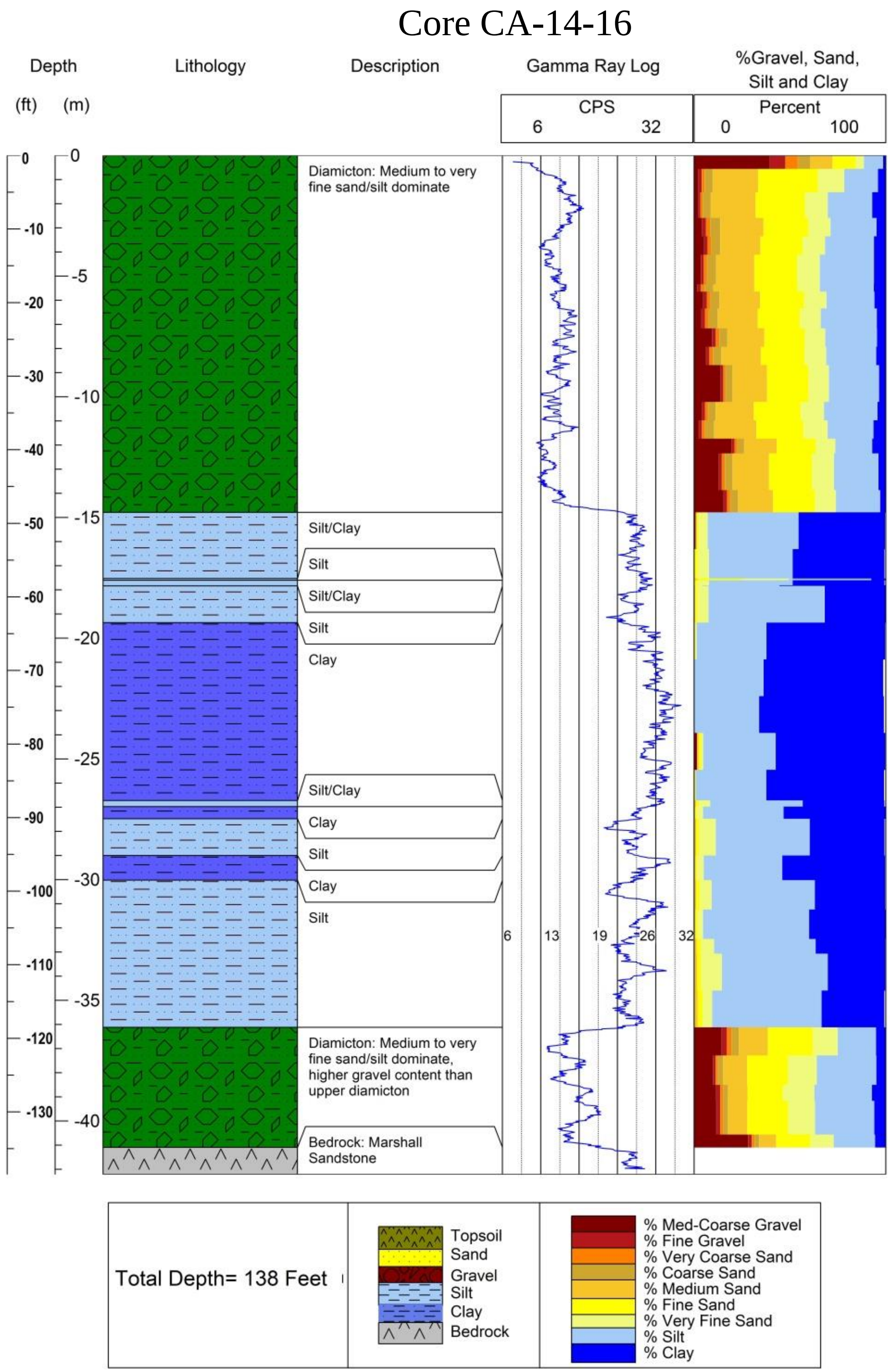

Figure 9. Logplot diagram of core CA-14-16. Shows lithology, gamma ray signature, and grain size distribution. The core contains two diamicton units separated mainly by silt and clay.

Table 3

Core CA-14-16 Lithology Results (%)

Lithology	Shale		Mafic		Felsic		Quartzite		Quartz Grain		Clastic		Limestone / Dolomite	
Sample	**Sieve #10**	**Sieve #18**	**Sieve #10**	**Sieve #18**	**Sieve #10**	**Sieve #18**	**Sieve #10**	**Sieve #18**	**Sieve #10**	**Sieve #18**	**Sieve #10**	**Sieve #18**	**Sieve #10**	**Sieve #18**
0-5 A (1)	2	6	6	1	19	34	10	9	14	19	10	12	39	20
5-8.5 A	6	11	10	7	34	29	30	17	12	26	9	10	0	0
8.5-18.5 B	4	1	13	7	20	31	23	16	11	10	6	6	23	29
18.5-28.5 B	4	4	7	2	25	39	18	15	4	13	9	6	32	21
28.5-38.5 C	5	2	18	8	13	31	29	22	6	16	1	0	28	22
38.5-48.5 C	6	4	10	9	16	22	25	19	5	19	4	6	33	21
118.5-128.5 A	1	1	6	5	9	13	10	4	17	22	32	29	25	26
118.5-128.5 B	7	3	5	4	9	10	5	7	7	27	38	31	28	18
Average	4	4	9	5	18	26	19	14	10	19	14	12	26	20

Note: Numbers represent percentages of a specified lithology for each sample. Light grey lines separate upper, middle, and lower sample groupings in the core.

Channelized Lowland: Inside of St. Joseph Sluiceway

Core CA-14-10

Core Ca-14-10 is located inside the St. Joseph sluiceway (refer to Figure 8). Stratigraphy of the core consists mostly of dark gray to black sand and gravel. Total depth of the core is 67.5 feet. Bedrock underlying this core is the Coldwater Formation, which consists mostly of shale. Complete textural analysis is completed for this core (Figure 10).

Core CA-14-10, on average, has high percentages of limestone/dolomite, felsic, and quartzite grains (Table 4). Average shale lithology is the lowest percentage in the core (Table 4). The entire core is characterized by sand and gravel with a normalized texture of 90.03% sand, 2.42% silt, and 0.54% clay (Figure 10).

Table 4 indicates that there is a difference between the size fractions of 1-2 mm (#18) and 2-4 mm (#10) grains. Overall, felsic, quartzite, and limestone/dolomite groupings display a higher percentage in the 2-4 mm (#10) size fraction. Shale, mafic, quartz grains, and clastic lithologies have a higher percentage of the 1-2 mm (#18) size fraction.

Overall, mafic, felsic, quartzite, clastic, and limestone/dolomite groupings have a higher percentage in the 2-4 mm (#10) size fraction. Quartz grains and shale rock fragments display a higher percentage in the 1-2 mm (#18) size fraction.

Core CA-15-05

Core CA-15-05 is located within the St. Joseph sluiceway (refer to Figure 9). Stratigraphy of the core consists mostly of dark gray to black sand and gravel. The total depth of the core is 50 feet. Bedrock underlying this core is the Coldwater Formation, which consists mostly of shale. Complete textural analysis was not completed for this core.

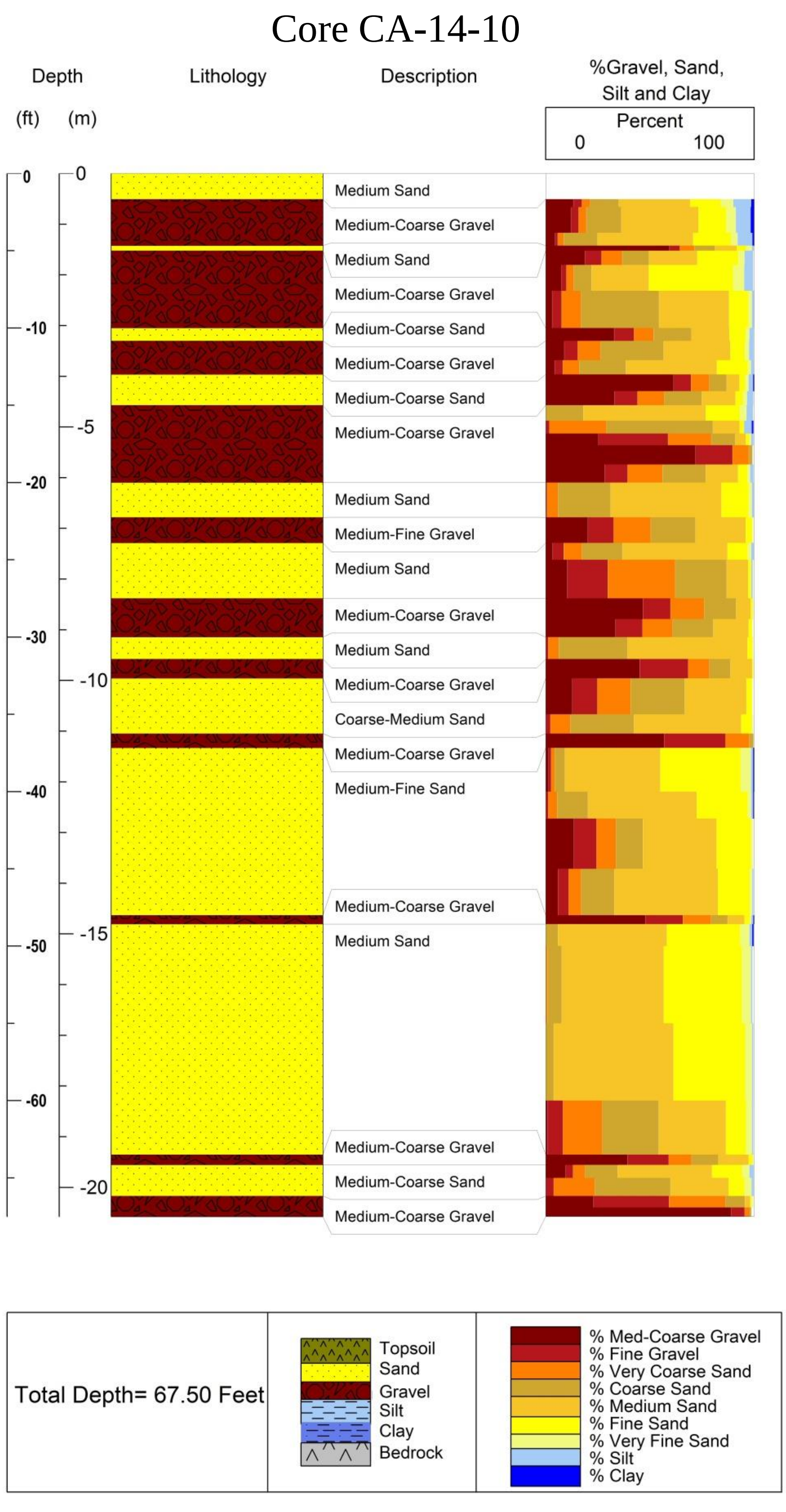

Figure 10. Logplot diagram of core CA-14-10. Shows lithology and grain size distribution. The core consists entirely of sand and gravel.

Table 4

Core CA-14-10 Lithology Results (%)

Lithology	**Shale**		**Mafic**		**Felsic**		**Quartzite**		**Quartz Grain**		**Clastic**		**Limestone / Dolomite**	
Sample	**Sieve #10**	**Sieve #18**	**Sieve #10**	**Sieve #18**	**Sieve #10**	**Sieve #18**	**Sieve #10**	**Sieve #18**	**Sieve #10**	**Sieve #18**	**Sieve #10**	**Sieve #18**	**Sieve #10**	**Sieve #18**
0-5 (4)	8	6	3	4	16	13	20	20	6	29	2	2	45	25
10-15 (2)	7	7	9	7	11	10	12	11	5	25	7	2	49	38
15-20 (2)	9	12	1	4	29	20	23	9	3	12	2	4	34	40
15-20 (5)	9	10	8	6	17	12	24	18	4	19	2	4	36	32
20-25 (1)	10	8	2	4	18	19	29	19	1	20	8	9	31	22
35-40 (2)	5	13	12	19	15	21	17	4	10	15	9	13	33	16
40-45 (2)	5	6	15	11	21	20	8	8	9	20	17	16	25	19
65-67.5 (2)	5	13	12	19	15	21	17	4	10	15	9	13	33	16
Average	7	9	8	9	18	17	19	12	6	19	7	8	36	26

Note: Light grey lines separate upper, middle, and lower sample groupings in the core.

Lithology results for the core are shown in Table 5. This core, on average, displays high percentages of limestone/dolomite and felsic material. The shale lithology group displays the lowest percentage in this core.

Table 5 indicates that there is a difference between the size fractions of 1-2 mm (#18) and 2-4 mm (#10) grains. Overall, mafic, felsic, quartzite, clastic, and limestone/dolomite groupings have a higher percentage in the 2-4 mm (#10) size fraction. Quartz grains and shale rock fragments display a higher percentage in the 1-2 mm (#18) size fraction.

Core CA-15-08

Core CA-15-08 is located within the St. Joseph sluiceway (refer to Figure 8). Stratigraphy of the core consists mostly of dark gray to black, sand and gravel. The total depth of the core is 58 feet. Bedrock underlying this core is the Coldwater Formation, which consists mostly of shale. Complete textural analysis was not completed for this core.

Lithology results for the core are shown in Table 6. This core, on average, displays high percentages of limestone/dolomite and felsic lithologies. Shale and quartz grain lithologic groupings display the lowest percentages in this core.

Table 6 indicates that there is a difference between the size fractions of 1-2 mm (#18) and 2-4 mm (#10) grains. Overall, mafic, felsic, quartzite, clastic, and limestone/dolomite groupings display a higher percentage in the 2-4 mm (#10) size fraction. Quartz grains and shale lithologies display a higher percentage in the 1-2 mm (#18) size fraction.

Longitudinal Profiles and Map Results

Two profiles were created within the St. Joseph sluiceway, a: 1) longitudinal profile along the traceable boundaries (Figure 11), and 2) terrace profile based on identified terrace surfaces within the sluiceway (Figure 12).

Table 5

Core CA-15-05 Lithology Results (%)														
Lithology	**Shale**		**Mafic**		**Felsic**		**Quartzite**		**Quartz Grain**		**Clastic**		**Limestone / Dolomite**	
Sample	**Sieve #10**	**Sieve #18**	**Sieve #10**	**Sieve #18**	**Sieve #10**	**Sieve #18**	**Sieve #10**	**Sieve #18**	**Sieve #10**	**Sieve #18**	**Sieve #10**	**Sieve #18**	**Sieve #10**	**Sieve #18**
10-15	6	3	20	9	22	24	18	18	4	15	11	13	19	18
15-20	11	13	13	11	25	22	17	9	6	20	8	12	21	14
20-25	10	17	19	8	14	10	18	6	1	37	14	17	25	5
25-30	4	16	13	7	12	10	8	15	4	17	27	10	32	26
30-35	12	14	14	8	20	23	16	8	4	11	15	15	19	21
35-40	5	4	19	23	23	19	16	12	4	14	12	13	21	16
45-50	9	13	15	20	27	24	6	5	2	15	11	8	30	15
Average	8	11	16	12	21	19	14	10	4	18	14	12	24	17

Note: Light grey lines separate upper, middle, and lower sample groupings in the core.

Table 6

Core CA-15-08 Lithology Results

Lithology	Shale		Mafic		Felsic		Quartzite		Quartz Grain		Clastic		Limestone / Dolomite	
Sample	**Sieve #10**	**Sieve #18**	**Sieve #10**	**Sieve #18**	**Sieve #10**	**Sieve #18**	**Sieve #10**	**Sieve #18**	**Sieve #10**	**Sieve #18**	**Sieve #10**	**Sieve #18**	**Sieve #10**	**Sieve #18**
5-10	6	13	20	11	16	18	15	12	1	15	18	15	25	14
10-15	6	18	10	5	15	23	23	8	1	6	15	18	30	22
25-30	9	20	10	15	21	17	13	11	3	10	18	12	27	15
30-35	7	13	15	11	9	16	11	13	3	13	15	11	41	24
40-45	-	34	-	3	-	23	-	14	-	4	-	7	-	15
45-50	5	13	13	6	23	15	9	6	2	10	17	19	32	31
Average	7	18	13	9	17	19	14	11	2	10	16	14	31	20

Note: Light grey lines separate upper, middle, and lower sample groupings in the core. Dashes indicate a lack of sample for that sieve fraction.

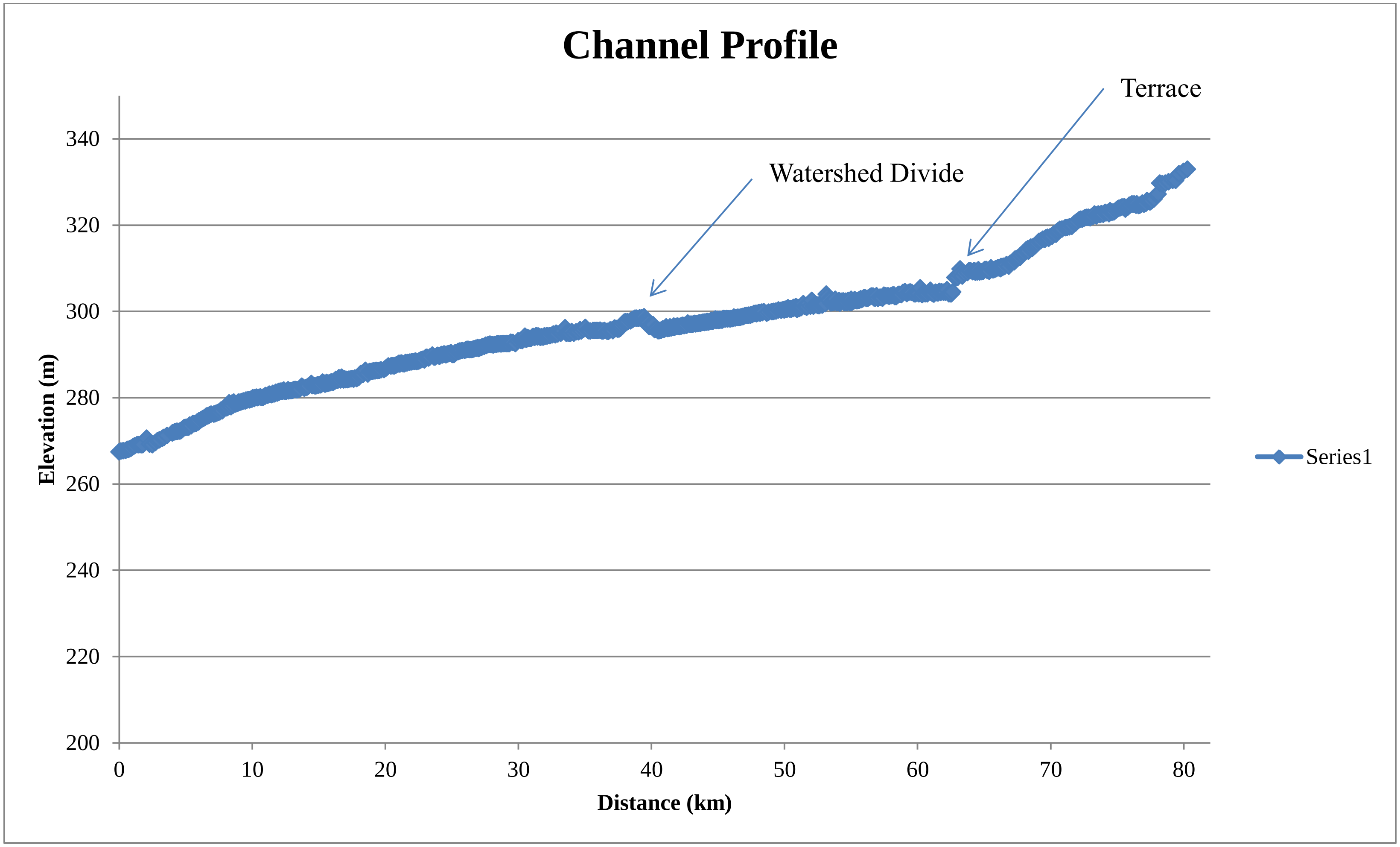

Figure 11. Longitudinal profile of the St. Joseph sluiceway. Two notable disruptions occur at about 40 km and 60 km along the profile.

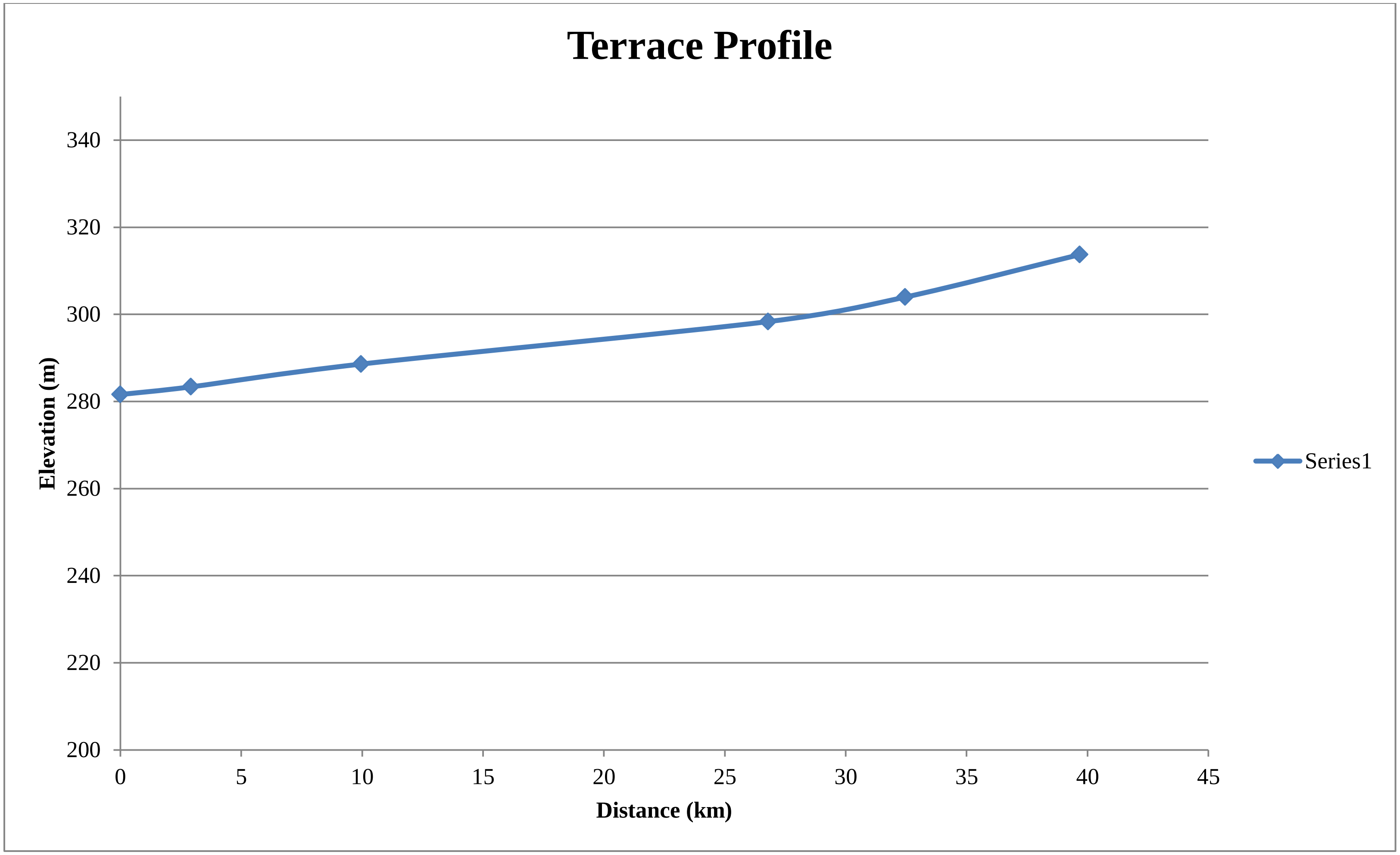

Figure 12. Longitudinal profile of the terrace deposits within the St. Joseph sluiceway.

The extent of the longitudinal profile, the location of the terraces, and a detailed example of terraces can be found in Figures 13, 14, and 15 respectively.

The longitudinal profile of the St. Joseph sluiceway shows a smooth, continuous gradient decreasing from east to west. There are two slight disruptions in the profile (refer to Figure 11). The first is located toward the eastern end of the sluiceway. There is a sudden fall in the profile where the modern stream passes through a terrace deposit. This fall resembles a knickpoint (Figure 16).

The second disruption is located further west along the sluiceway. It is caused by the current watershed divide between the St. Joseph River watershed and the Kalamazoo River watershed. This is due to stream capture, in which the southern branch of the Kalamazoo River is diverted (captured) from the St. Joseph sluiceway toward the Kalamazoo main channel. This diversion could be caused by greater discharge and downcutting of the Kalamazoo River ultimately developing the watershed divide.

Six terrace deposits were also used to create a profile within the St. Joseph sluiceway (refer to Figures 11, 14 and 15). The terrace profile displays a smooth continuous gradient from east to west. The terrace deposits represent an early channel bed that was later down-cut. The down cutting may have been caused by a change in either fluvial discharge or sediment supply coming from the Huron-Erie lobe. Additionally, a change in base level at the downstream end of the St. Joseph sluiceway could also account for the down cutting (Benn and Evans, 2010).

The St. Joseph sluiceway is one of many channels observed throughout the area. The channels are delineated in a regional channel-flow-direction map created for the area immediately surrounding the St. Joseph sluiceway (Figure 17). This map was created by tracing sluiceway scarps to delineate the channels.

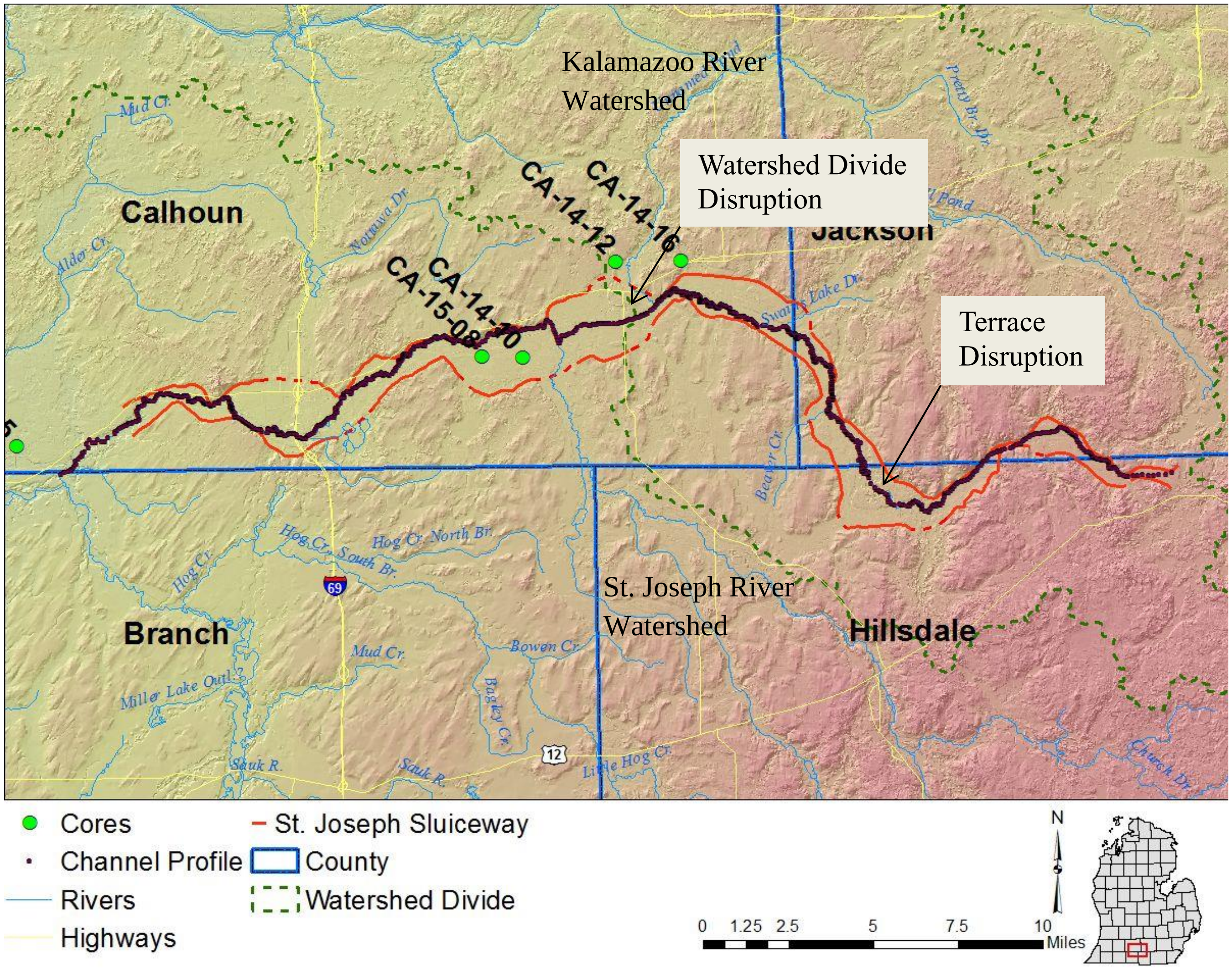

Figure 13. Location of St. Joseph sluiceway longitudinal profile disruptions.

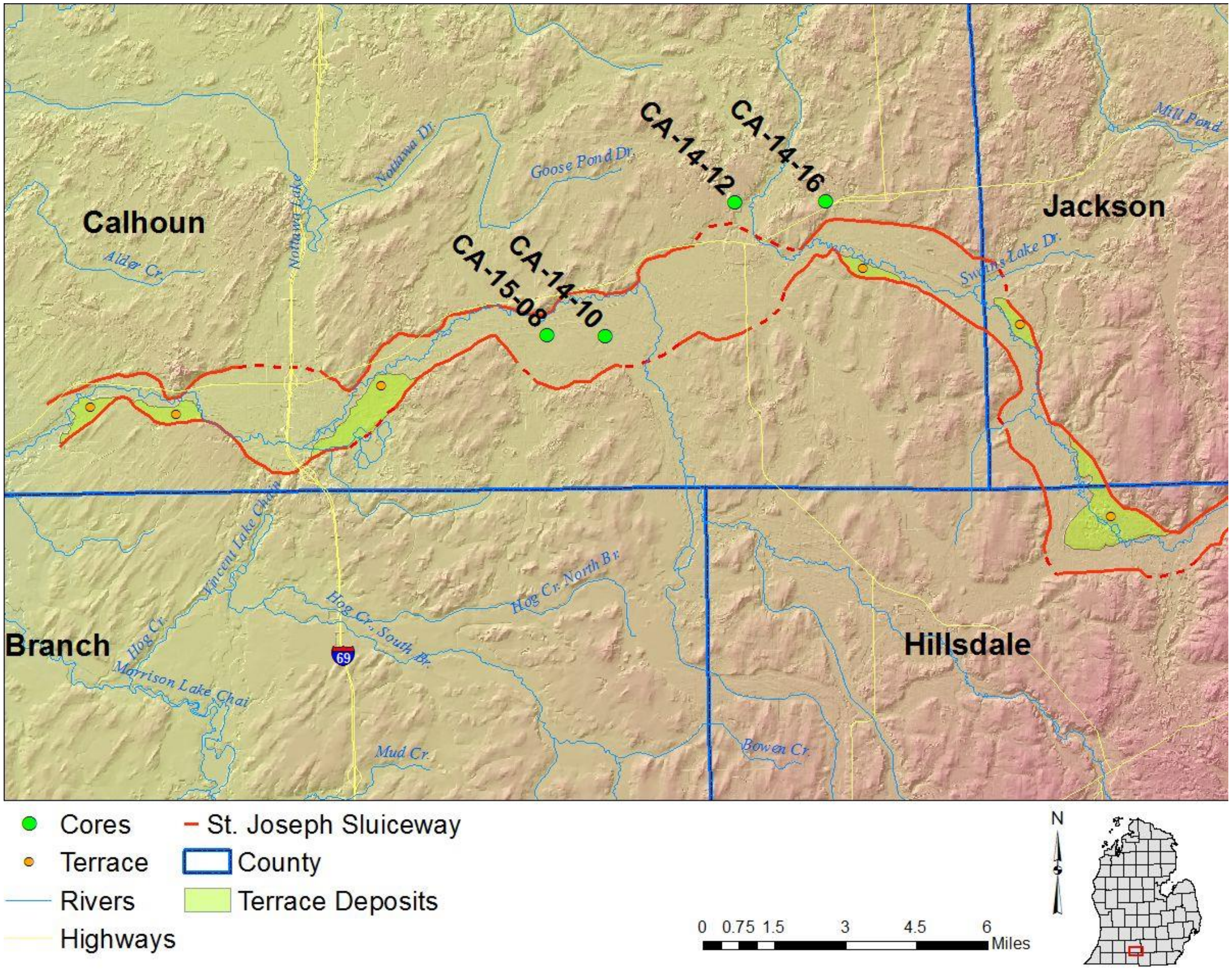

Figure 14. Location of terrace deposits in the St. Joseph sluiceway.

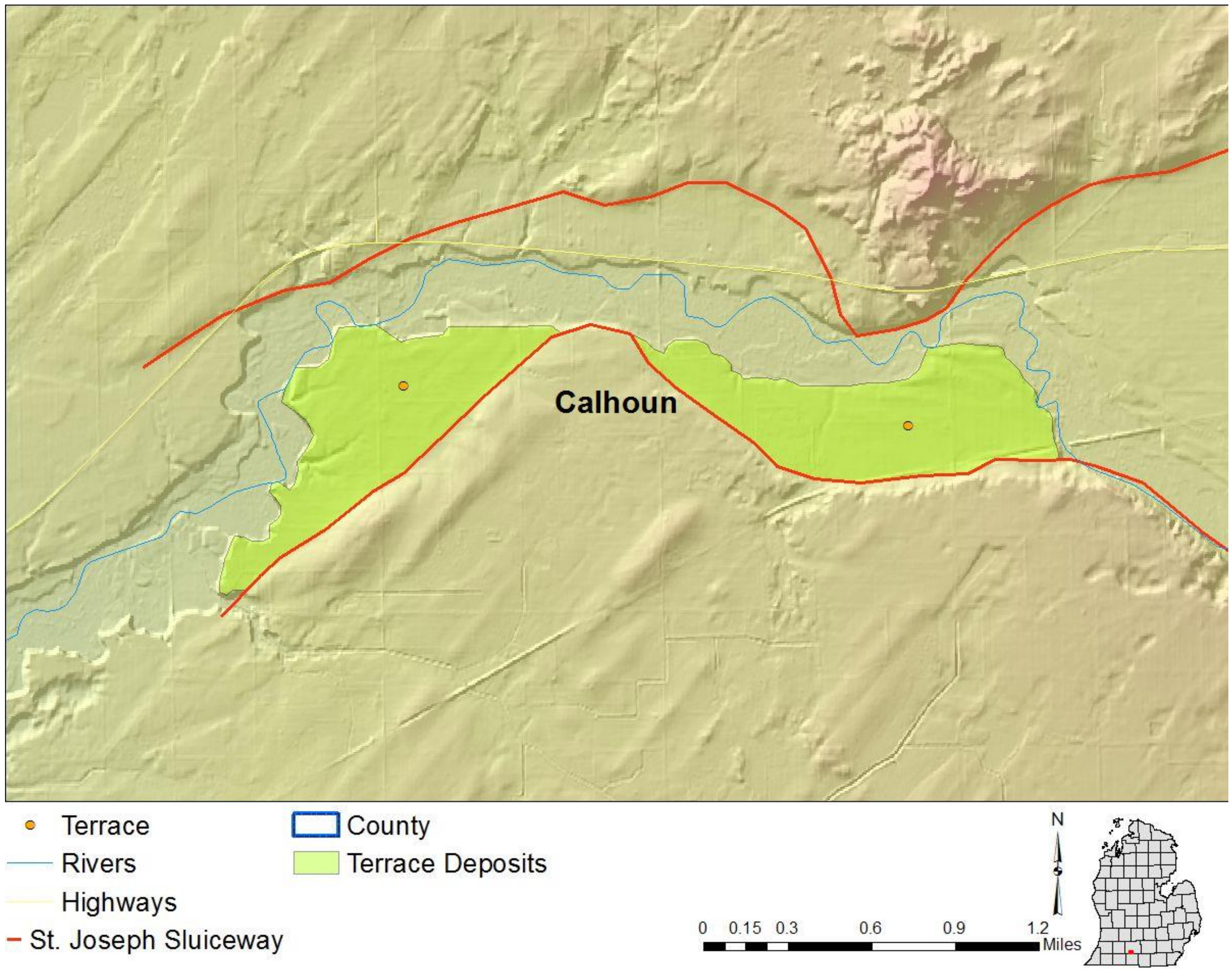

Figure 15. Detailed view of select terraces.

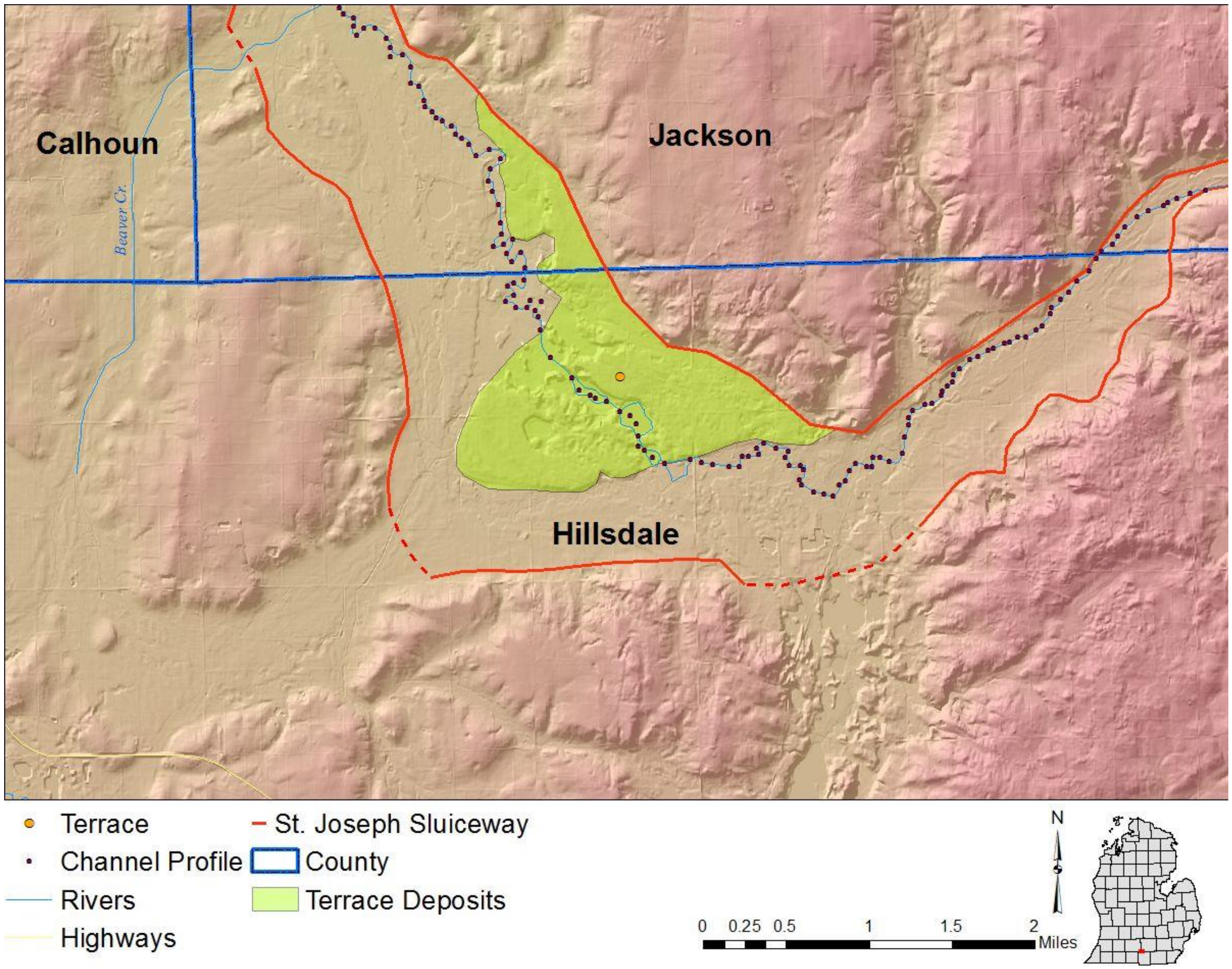

Figure 16. Modern stream flowing through a terrace deposit.

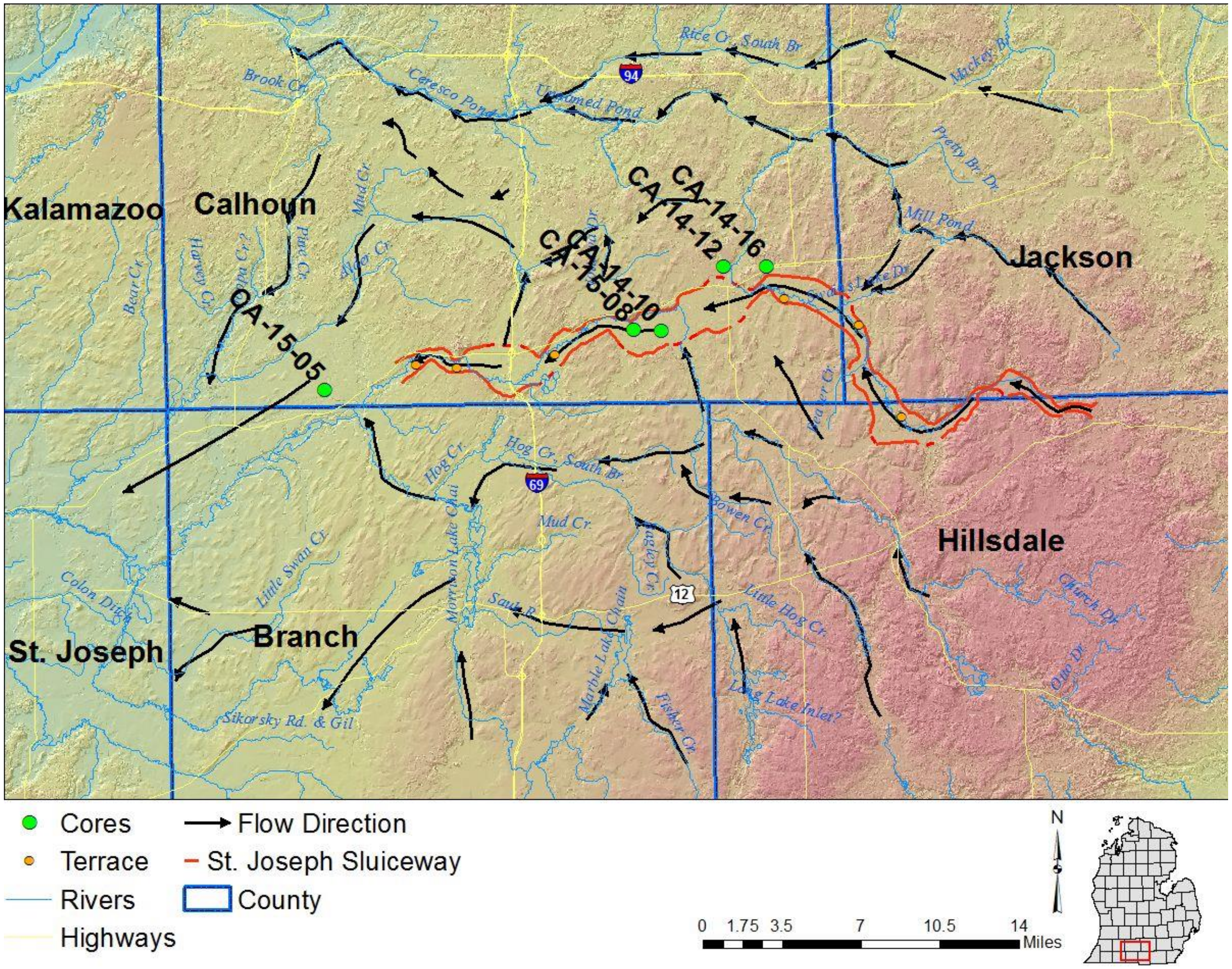

Figure 17. Flow direction within identified channels throughout the study area. Flow direction was established by creating profiles within each channel. Each arrow indicates a flow direction for a single channel. Note the general NE to SW flow pattern.

After a channel was identified, and delineated, a general profile was created for each channel to determine flow direction. This map showed a general northeast to southwest flow direction for the channel network.

CHAPTER V

DISCUSSION

One major goal of this study was to determine if there is a difference in ice lobe sediment source between the drumlinized uplands and the adjacent channelized lowlands in the study area. Evidence supporting a different ice lobe origin for the two landform types includes: 1) grain size analysis of texture in the complete core profiles, 2) sand-grain lithology results, 3) flow direction of longitudinal profiles, and 4) regional network of channels.

Grain-Size Analysis

Grain size analysis and texture indicate a difference between the drumlinized uplands and the St. Joseph sluiceway. The stratigraphy of core CA-14-16, located in the drumlinized uplands of the study area, has an upper and lower diamicton unit separated by a silt/clay unit. The drumlins are oriented in a NE-SW direction suggesting they were formed by Saginaw lobe ice. The lithology results indicated a difference in the amount of clastic grains between the upper and lower till units described in the complete core profile (refer to Figure 9). The difference suggests that there was a change in the amounts of local bedrock being incorporated into the Saginaw ice lobe. Increased amounts of clastic grains suggest more erosion and deposition of local bedrock; whereas, the limited amount in the upper till suggests a change to the recycling of previously eroded material.

Grain size analysis and texture of core CA-14-10 (refer to figure 10), located inside the St. Joseph sluiceway, is predominately sand and gravel. The sand and gravel texture indicates a different mode of deposition than the diamicton texture in the upland core, CA-14-16. This sand and gravel texture indicates an environment of deposition interpreted to be an outwash deposit.

The diamicton texture, in contrast, represents a till that is interpreted to be deposited in contact with ice.

Texture differences observed in the core profiles of CA-14-10 and CA-14-16 are also observed in the other three cores used in this study. Cores located within the St. Joseph sluiceway (cores CA-14-10, CA-15-05, and CA-15-08) are darker in color and are composed almost entirely of sand and gravel; whereas, cores from outside the St. Joseph sluiceway (cores CA-14-12 and CA-14-16) are lighter in color (typically tan to light brown) and have a texture ranging from diamicton to silts/clays (Table 7 and Figure 18).

Core CA-14-10, of the St. Joseph sluiceway (mentioned above), when compared to core CA-14-12, of the drumlinized upland, both display a similar texture of sand and gravel. The sand and gravel texture of both are consistent with outwash deposits. CA-14-10 displays a dark gray to black color whereas core CA-14-12 displays a tan to light brown color.

This color difference is significant because it suggests a difference in lithology between to two cores. The observed difference in color is interpreted as being derived from different lithology sources. Darker lithologies are thought to be derived from the Huron-Erie lobe, which overrode more shale formations in the southeast Michigan Basin. Lighter lithologies are interpreted to be derived from the bedrock underlying the Saginaw lobe, which overrode more sandstone formations near the center of the Michgan Basin.

Table 7
Core Texture Comparison

Core	**Location**	**Texture**	**Color**	**Depositional Environment**
CA-14-12	Drumlinized Upland	Sand/Gravel	Light	Outwash
CA-14-16	Drumlinized Upland	Diamicton	Light	Ice Deposited Till
CA-14-10	St. Joseph sluiceway	Sand/Gravel	Dark	Outwash
CA-15-05	St. Joseph sluiceway	Sand/Gravel	Dark	Outwash
CA-15-08	St. Joseph sluiceway	Sand/Gravel	Dark	Outwash

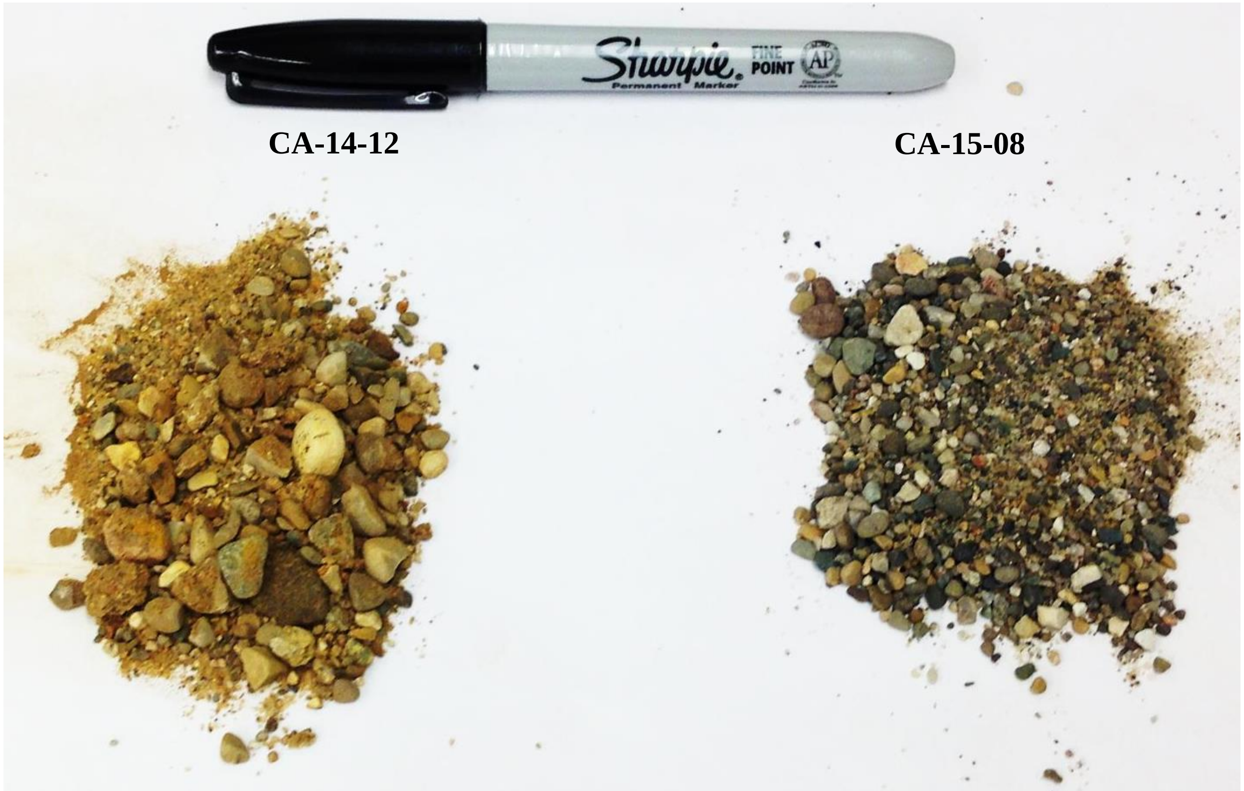

Figure 18. Color difference between samples from cores CA-14-12 and CA-15-08. Note the darker color of the core CA-15-08 (right) compared to the lighter color of CA-14-12 (left). Samples were collected from the 45-50 ft interval for each core.

Lithology Interpretation

Sand-grain lithology provides the most striking evidence in support of different lobe sources for the sluiceway versus drumlinized upland deposits. To test if a certain grain lithology was significantly more or less abundant in the drumlinized upland vs the sluiceway, two groups of samples were created based on the locations of the cores. The inside group represents cores within the St. Joseph sluiceway (also referred to as the channelized lowlands) and the outside group represents cores obtained from the drumlinized uplands (outside the St. Joseph sluiceway).Samples were taken from the upper, middle and lower intervals in each core (not from correlated stratigraphic units) to represent the overall lithology of each core (refer to methods chapter). This sampling procedure facilitated the comparison of relative depths

between the inside (St. Joseph sluiceway) and outside groups (drumlinized upland) as mentioned above. Several t-tests were conducted to determine what significant differences exist between the inside and outside groupings. The following are the results of each t-test conducted and an interpretation of those results.

Lithology T-tests

T-tests are used to test whether the mean of a population differs from the mean of another population. This study uses both two- and one-tailed t-tests in order to determine significant difference between the channelized areas and the drumlinized areas. Two-tailed t-test simply determines if there is a significant difference between two populations; whereas, a one-tailed t-test can test if one population is greater or less than another population. Two-tailed t-tests are used to determine if the null hypothesis (H_0: X_1-X_2=0) or an alternative hypothesis (H_1: X_1-$X_2 \neq 0$) is true. X_1 is the mean of population 1 and X_2 is the mean of population 2. The mean, standard deviation, and standard error are used to calculate a t-calculated value using the equation $t = \frac{\bar{X}1 - \bar{X}2}{\sqrt{\frac{s_1}{n_1}+\frac{s_2}{n_2}}}$ where: $\bar{X}_1$ and $\bar{X}_2$ are the means of populations one and two respectively, S_1 and S_2 is the standard deviation of populations one and two respectively, and n_1 and n_2 are the number of observation for populations one and two respectively. The t-calculated value is then compared to a tabulated t-critical value found by using the calculated degrees of freedom ($d.f. = n_1 + n_2 - 2$) and the chosen alpha (α) value (or confidence level). If t-calculated is greater than t-critical, then the null hypothesis is rejected (or we must accept the alternative hypothesis), indicating a significant difference between the two populations. The one-tailed t-test concerns only one side (or tail) of a distribution. The one-tailed t-test is used to determine if the null hypothesis (H_0: X_1-X_2=0) or an alternative hypothesis (H_0: X_1-$X_2 \geq 0$) is true. The

alternative hypothesis of a one-tailed t-test tests whether one population is larger or smaller (depending on which tail is used) than another population. This is unlike the two-tail test, which simply determines if two populations are different. One-tailed t-tests also compare a t-calculated value to a t-critical value in order to accept one of the hypotheses. When t-calculated is greater than the t-critical value, then the alternative hypothesis is accepted. T-tests in this study were conducted using Minitab software. Results of the t-tests can be found in Appendix A.

All t-tests referred to in this study are comparing the inside (inside the St. Joseph sluiceway) and outside (drulinized upland area) grouping of cores. The first statistical analysis completed was a two-tailed t-test comparing inside and outside grouping for the bulk, #10 (2-4 mm), and #18 (1-2 mm) sieve fractions. A two-tailed t-test was also completed for the upper, middle, and lower for the #10 (2-4 mm) and #18 (1-2 mm) sieve fractions. This test was done to determine if there was a significant difference between the inside and outside groupings. One-tailed t-tests were also conducted for all of the above-mentioned groupings to determine if the inside or outside grouping was more plentiful in a specific lithology. Results for these tests are presented in Figure 19 and Figure 20 for each lithology group and discussed in the following paragraphs.

Shale Lithology

The shale lithology group showed a significant difference in the two-tailed t-test in the bulk, #10, and #18 size fractions. Results of the one-tail t-test showed that shale was more plentiful for the inside grouping. The subgroups of upper, middle, and lower showed mixed results in the two-tailed t-test, but were consistent in the one-tailed t-test, showing the inside grouping as having a higher shale content. Upper and middle subgroupings were significantly different within a two-tailed t-test between the inside and outside groupings.

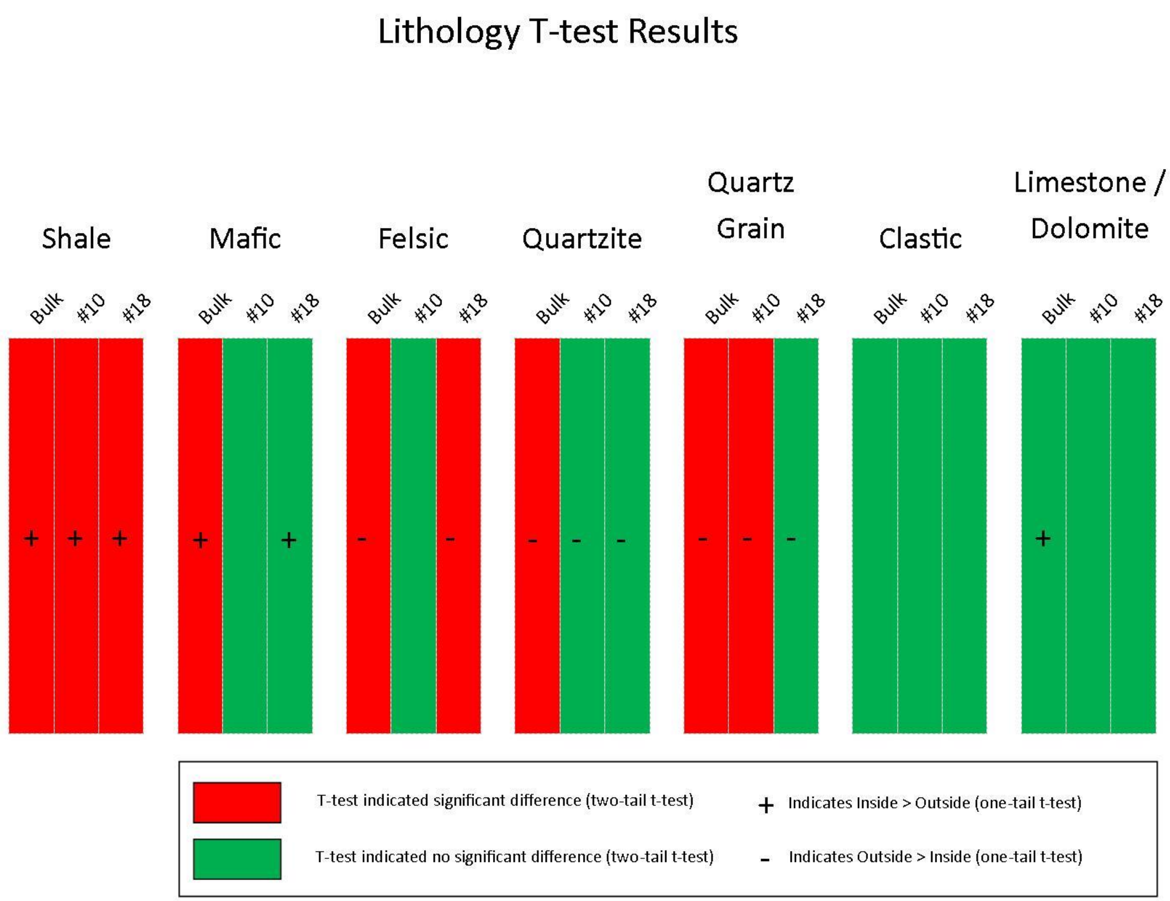

Figure 19. Lithology t-test results for bulk samples and #10 and #18 size fractions. Two-tail t-test results were used to test if there is a significant difference between the Inside and Outside groups. The one-tailed t-test was used to test whether the Inside group has a higher percentage lithology than the Outside group.

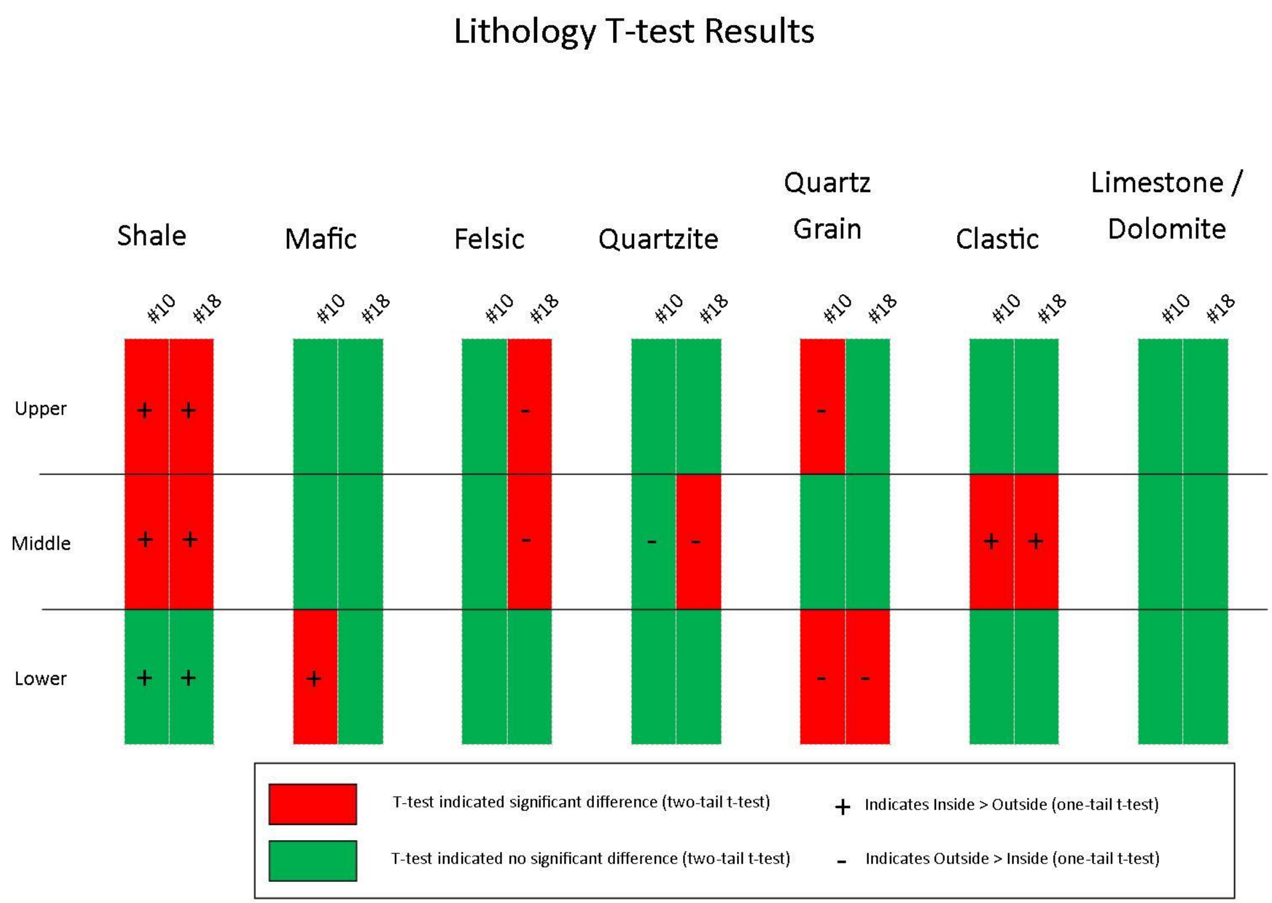

Figure 20. Lithology t-test results for #10 and #18 size fractions. Two-tail t-test results were used to test if there is a significant difference between the Inside and Outside groups. The one-tailed t-test was used to test whether the Inside group has a higher percentage lithology than the Outside group.

The one-tailed t-test results showed that shale content was significantly more abundant in all of the subgroupings (upper, middle, and lower).

It is interpreted that the increased shale content for the inside group most likely comes from Paleozoic bedrock underlying the Huron-Erie lobe flow path.

The Huron-Erie lobe, being the meltwater source for the St. Joseph sluiceway, overrode several shale bearing formations in the southeastern Michigan Basin. This shale would have been incorporated into the Huron-Erie lobe ice as it passed over the formations. The bedrock distribution underlying the Huron-Erie lobe (refer to Figures 2 and 3) shows the location of shale-bearing formations (Coldwater, Antrim, Sunbury, Bedford) that are thought to have contributed to the shale lithology in the sluiceway.

Mafic Lithology

The two-tailed t-test for the mafic lithology group showed mixed results. The bulk sample showed a significant difference, but the difference between #10 and #18 sieve fractions for the inside and outside groupings was not significant. The one tailed t-test results showed that there were higher amounts of mafic material in the inside grouping for the bulk and #18 sieve fractions. The #10 sieve fractions showed no difference in the one-tailed t-test.

The similarity of the mafic lithology between the inside (St. Joseph sluiceway) and outside (drumlinized upland) groupings is interpreted to be due to the lack of local mafic bedrock. Mafic grains would have been far traveled to be deposited in the study area by the Sanginaw and Huron-Erie lobes; therefore, the amount of mafic lithology in the two lobes should be relatively similar.

Felsic Lithology

Two-tailed t-test results for the felsic lithology group were mixed. Two-tailed t-test results showed that the bulk and #18 sieve fractions were significantly different, but #10 sieve fractions were not significantly different. Upper and middle subgroupings for the #18 sieve fraction were the only significantly different subgroupings, whereas the other fractions showed no significant differences between the means of the inside and outside groupings. The one-tailed t-test results followed the same pattern as the two-tailed results. The bulk, #18 sieve fraction, and the upper/middle #18 sieve fraction showed a larger amount of felsic material in the outside grouping.

The greater amount of felsic material is interpreted to be derived from Paleozoic bedrock underlying the Saginaw lobe flow path. Distribution of bedrock underlying the Saginaw lobe (refer to Figure 2), indicates that there are more sandstones in this area than in the flow path of the Huron-Erie lobe. Therefore, the increased amount of felsic lithology is interpreted to reflect felsic clasts contained in and eroded from the sandstones underlying the Saginaw lobe flow path.

Quartzite Lithology

The two-tailed t-test results for the quartzite lithology group showed a significant difference only in the bulk sample and the middle subgroup #18 sieve fraction. The one-tailed t-test results indicated that the outside grouping had higher quartzite percentages in the bulk, #10, and #18 size fractions (Figure 19). The middle subgroup consisting of #10 and #18 sieve fractions (Figure 20) also indicated higher quartzite percentages in the outside group. All other subgroups showed no significant difference with either two-tailed or one-tailed t-tests.

Increased amounts of quartzite material are most likely derived from the Precambrian Lorrain Formation underlying the Saginaw lobe flow path. This formation has been established

as an indicator lithology for the Saginaw lobe (Anderson, 1957). Lorrain Formation outcrops are present along the northern shoreline of Lake Huron between Sault St. Marie and Elliot Lake, Ontario. The locations of these outcrops are directly within the former Saginaw lobe flow path but are not present under the former Huron-Erie lobe flow path.

Quartz Grain Lithology

The t-test results for the quartz grain lithology group had mixed results. Two-tailed t-test results showed a significant difference in the bulk, #10, upper #10, and lower #10 and #18 subgroups. One-tailed t-test results indicated increased amounts of quartz grain lithologies in the outside grouping for the bulk, #10, #18, upper #10, and lower #10 and #18 subgroups. All remaining subgroups showed no significance in either the one-tailed or the two-tailed t-tests.

The higher amounts of quartz grain clasts in the outside grouping are thought to be derived from the Paleozoic bedrock underlying the Saginaw lobe flow path. Similar to the felsic lithology grouping above, increased quartz grain lithology is derived from the increased amount of sandstone -bearing formations underlying the former Saginaw lobe.

Clastic Lithology

The t-tests for the clastic lithology group showed significance only in the middle #10 and #18 sieve fractions. Two-tailed t-test results showed a significance difference for only the middle #10 and #18 sieve fractions. The same subgrouping and sieve fractions showed a higher amount of clastic material in the inside grouping.

There is a greater amount of clastic lithology present in the lower till (as compared to the upper till) of core CA-14-16 (Table 3). This is most likely the result of more local bedrock erosion from the ice depositing the lower till. When the upper till was deposited, the bedrock

would have been buried under previously eroded and deposited sediments causing less erosion and deposition of local bedrock.

Limestone/Dolomite Lithology

The two-tailed t-test conducted for the limestone/dolomite lithology group showed no significant difference. The only one-tailed t-test result showing any significance was the middle #10 sieve fraction, indicating increased amounts of limestone/dolomite for the inside group.

Similar amounts of limestone/dolomite lithology between the inside and outside groupings occur because of the large amount of calcareous lithologies throughout the Michigan Basin. Many of the formations within the Michigan Basin contain calcareous units and therefore a large difference should not be expected. Although no significant lithologic difference was apparent in this study the limestone/dolomite group may have contributed to the color difference observed between the two classes of cores. Due to the lack of overwhelming amounts of mafic and shale lithologies inside the St. Joseph sluiceway, an additional source of darker material could be contributing to the color difference between the inside and outside channel deposits. It is possible that the carbonate lithologies in the path of the Huron-Erie lobe are darker in color that those along the Saginaw lobe flow path. This hypothesis could help explain the color difference observed.

Lithology Conclusion

Sand-grain lithology t-test results reveal much about the difference between the channelized lowland (inside the St. Joseph sluiceway) and the drumlinized upland (outside of the St. Joseph sluiceway) landforms areas in this study. These t-test results indicate that the shale lithology group has the strongest affiliation to the channelized landform (inside the St. Joseph sluiceway) than any other lithology. Shale lithology is consistently greater in all size fractions,

and depth categories tested in this study. These results combined with flow path and bedrock data indicate that the St. Joseph sluiceway was formed by meltwater from the Huron-Erie lobe.

Felsic, quartzite, and quartz grain lithologies display an affiliation to the drumlinized upland areas (outside of the St. Joseph sluiceway). These lithologies are derived from Paleozoic bedrock underlying the former Saginaw lobe and support the interpretation that the drumlinized uplands are Saginaw lobe derived.

Longitudinal Profile Interpretation

Longitudinal profiles of the St. Joseph sluiceway and the terrace deposits indicate a meltwater source from the Huron-Erie lobe. Regional channel outlines through the study area show a complicated network of meltwater flow paths resembling a braided network of channels. This braided network suggests main sources to the east and north of the study area.

The channel and terrace profiles created in this study show an east to west direction of flow within the St. Joseph sluiceway. Based on the approximate Huron-Erie lobe margin (Figure 21), an east to west flow direction suggests the meltwater source of the St. Joseph sluiceway to be from the Huron-Erie lobe.

Orientation of the braided network through the drumlinized uplands suggests that channels were created by a late meltwater event emanating from the Huron-Erie lobe. This late event eroded previous Saginaw lobe deposits in an east to west direction as it flowed away from the Huron-Erie lobe boundary.

Channels trending northeast southwest could be older tunnel valleys resulting from the Saginaw lobe. These channels, observed to be crosscut by the east-west channels (Figure 22), further indicating the east-west channels are a later event.

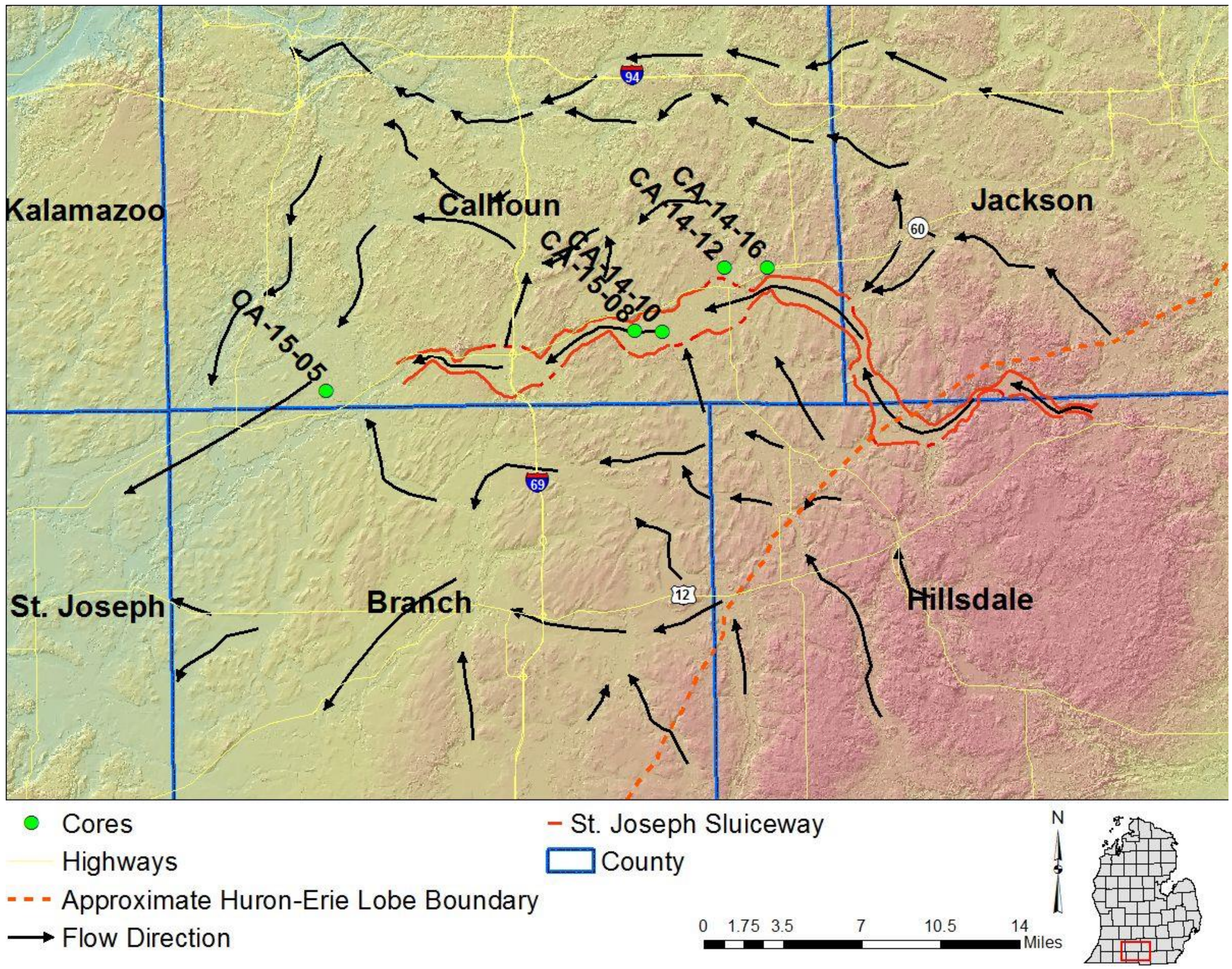

Figure 21. Huron-Erie lobe margin and flow direction map. Note the flow direction arrows toward the east tend to originate near the approximate Huron-Erie lobe boundary.

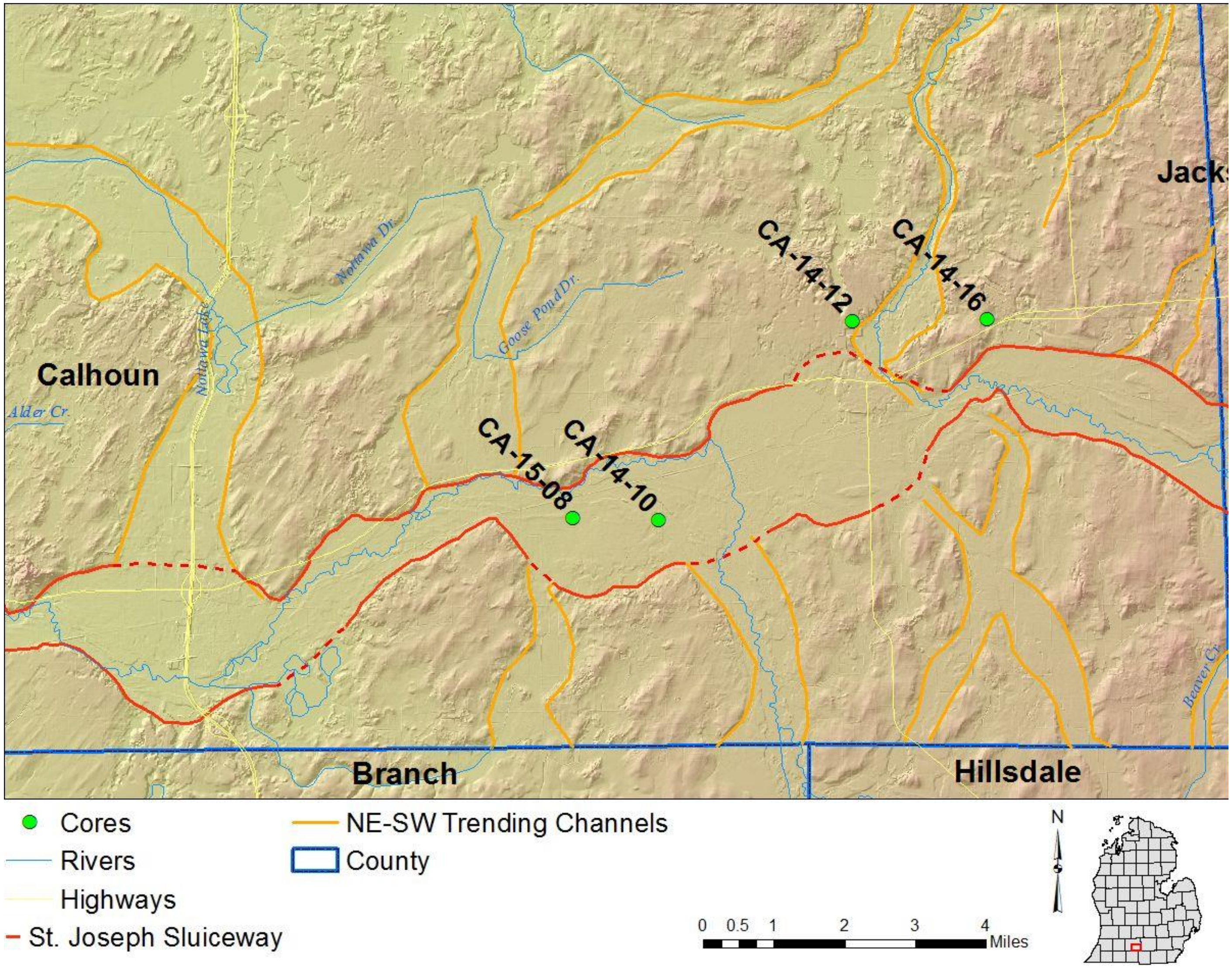

Figure 22. Outlines of the St. Joseph sluiceway and other channels in the study area. Note specifically how the St. Joseph sluiceway crosscuts the NE-SW trending channels.

CHAPTER VI

CONCLUSIONS

Grain size analysis, sand grain lithology, and longitudinal profiles were used to investigate the difference between sediments in channelized (inside of St. Joseph sluiceway) and drumlinized (outside of the St. Joseph sluiceway) areas of southern Calhoun County and its surrounding areas. Five cores were analyzed using grain size analysis and sand grain lithology analysis in order to determine a difference between drumlimized and channelized deposits. Cores were chosen based on their location in either the drumlinized uplands or the channelized lowlands. Longitudinal profiles also aided in determining channel flow direction in the study area, and determining the upstream terminus of the St. Joseph sluiceway.

The findings of this study have brought new information to the delineation of interlobate boundaries in south central Michigan using grain size analysis. Grain size analysis results showed a difference in texture between the channelized (within the St. Joseph sluiceway) and the drumlinized (outside the St. Joseph sluiceway) areas. The channelized areas consistently displayed a texture of dark colored sand and gravel; whereas, the drumlinized areas displayed a texture ranging from light colored diamicton to silt/clay. These results suggest different modes of deposition for the two areas. The color difference points to different sediment source areas.

Sand grain lithology results show increased amounts of shale lithology within the St. Joseph sluiceway (channelized area). Lithology results also displayed increased amounts of felsic, quartzite, and quartz grain lithologies outside of the St. Joseph sluiceway (drumlinized area). The increased amount of shale grains in the St. Joseph sluiceway (derived from shale formations underlying the former Huron-Erie lobe) suggest a Huron-Erie lobe source. The

increased amount of felsic, quartzite, and quartz grain lithologies (derived from Paleozoic bedrock underlying the former Saginaw lobe) suggest a Saginaw lobe source.

Longitudinal profiles of the St. Joseph sluiceway and terrace deposits within the sluiceway display an east to west direction of flow suggesting a Huron-Erie lobe source. Longitudinal profiles of channels in the region surrounding the St. Joseph sluiceway have revealed a complicated network that broadly flows from the northeast to the southwest in the study area.

Appendix A
Lithology T-test Results

Shale:
Two Sample T-Test Results

Two-Tail	Bulk		#10		#18		#10 Upper		#18 Upper		#10 Middle		#18 Middle		#10 Lower		#18 Lower	
	Inside	Outside	Inside	Outside	Inside	Outside	Inside	Outside	Inside	Outside	Inside	Outside	Inside	Outside	Inside	Outside	Inside	Outside
N	41	32	20	16	21	16	8	6	8	6	8	5	8	5	4	5	5	5
Mean	10.02	3.47	7.36	3.67	12.55	3.26	7.69	4.26	10.19	4.27	7.72	3.87	13.23	2.6	5.98	2.77	15.2	2.73
StDev	5.67	2.57	2.37	2.2	6.73	2.95	1.82	2.36	4.85	4.64	2.97	1.64	4.66	1.34	2.02	2.62	11.2	1.23
SE Mean	0.89	0.45	0.53	0.55	1.5	0.74	0.64	0.96	1.7	1.9	1.1	0.73	1.6	0.6	1	1.2	5	0.55
C.I.	4.557, 8.543		2.134, 5.240		5.92, 12.65		0.81, 6.05		0.30, 11.54		0.99, 6.71		6.58, 14.67		-0.58, 6.98		-1.49, 26.53	
t-Calc.	6.58		4.83		5.65		2.96		2.32		3		6.06		2.07		2.48	
t-Crit.	2		2.042		2.048		2.262		2.201		2.228		2.306		2.447		2.776	
P-Value	0		0		0		0.016		0.041		0.013		0		0.084		0.068	
DF	58		33		28		9		11		10		8		6		4	
Accept/Reject	Reject		Reject		Reject		Reject		Reject		Reject		Reject		Accept		Accept	
Alternate Hyp.	Inside-Outside ≠ 0		Inside-Outside ≠ 0		Inside-Outside ≠ 0		Inside-Outside ≠ 0		Inside-Outside ≠ 0		Inside-Outside ≠ 0		Inside-Outside ≠ 0		Inside-Outside ≠ 0		Inside-Outside ≠ 0	

One-Tail	Bulk		#10		#18		#10 Upper		#18 Upper		#10 Middle		#18 Middle		#10 Lower		#18 Lower	
	Inside	Outside	Inside	Outside	Inside	Outside	Inside	Outside	Inside	Outside	Inside	Outside	Inside	Outside	Inside	Outside	Inside	Outside
N	41	32	20	16	21	16	8	6	8	6	8	5	8	5	4	5	5	5
Mean	10.02	3.47	7.36	3.67	12.55	3.26	7.69	4.26	10.19	4.27	7.72	3.87	13.23	2.6	5.98	2.77	15.2	2.73
StDev	5.67	2.57	2.37	2.2	6.73	2.95	1.82	2.36	4.85	4.64	2.97	1.64	4.66	1.34	2.02	2.62	11.2	1.23
SE Mean	0.89	0.45	0.53	0.55	1.5	0.74	0.64	0.96	1.7	1.9	1.1	0.73	1.6	0.6	1	1.2	5	0.55
C.I.	4.886		2.395		6.49		1.31		1.34		1.53		7.73		0.2		1.76	
t-Calc.	6.58		4.83		5.65		2.96		2.32		3		6.06		2.07		2.48	
t-Crit.	1.671		1.697		1.701		1.833		1.796		1.812		1.86		1.943		2.132	
P-Value	0		0		0		0.008		0.02		0.007		0		0.042		0.034	
DF	58		33		28		9		11		10		8		6		4	
Accept/Reject	Reject		Reject		Reject		Reject		Reject		Reject		Reject		Reject		Reject	
Alternate Hyp.	Inside-Outside > 0		Inside-Outside > 0		Inside-Outside > 0		Inside-Outside > 0		Inside-Outside > 0		Inside-Outside > 0		Inside-Outside > 0		Inside-Outside > 0		Inside-Outside > 0	

Mafic:
Two Sample T-Test Results

Two-Tail	Bulk		#10		#18		#10 Upper		#18 Upper		#10 Middle		#18 Middle		#10 Lower		#18 Lower	
	Inside	Outside	Inside	Outside	Inside	Outside	Inside	Outside	Inside	Outside	Inside	Outside	Inside	Outside	Inside	Outside	Inside	Outside
N	41	32	20	16	21	16	8	6	8	6	8	5	8	5	4	5	5	5
Mean	11.05	7.86	12.13	9.53	10.02	6.19	10.5	10.41	7.13	5.97	12.49	12.49	10.36	7.01	14.69	5.11	14.11	5.62
StDev	5.73	4.44	5.51	4.81	5.88	3.41	6.91	5.16	3.01	3.73	4.83	4.55	4.74	4.57	3.16	0.595	8.95	1.99
SE Mean	0.9	0.78	1.2	1.2	1.3	0.85	2.4	2.1	1.1	1.5	1.7	2	1.7	2	1.6	0.27	4	0.89
C.I.	0.82, 5.57		-0.90, 6.11		0.70, 6.98		-7.00, 7.20		-3.04, 5.36		-6.01, 6.00		-2.74, 9.44		4.09, 14.27		-2.89, 19.87	
t-Calc.	2.69		1.51		2.49		0.03		0.63		0		1.27		5.74		2.07	
t-Crit.	2		2.042		2.042		2.201		2.262		2.262		2.306		3.182		2.776	
P-Value	0.009		0.139		0.018		0.977		0.547		0.999		0.24		0.011		0.107	
DF	70		33		32		11		9		9		8		3		4	
Accept/Reject	Accept		Reject		Rejcet		Accept		Accept		Accept		Accept		Reject		Accept	
Alternate Hyp.	Inside-Outside ≠ 0		Inside-Outside ≠ 0		Inside-Outside ≠ 0		Inside-Outside ≠ 0		Inside-Outside ≠ 0		Inside-Outside ≠ 0		Inside-Outside ≠ 0		Inside-Outside ≠ 0		Inside-Outside ≠ 0	

One-Tail	Bulk		#10		#18		#10 Upper		#18 Upper		#10 Middle		#18 Middle		#10 Lower		#18 Lower	
	Inside	Outside	Inside	Outside	Inside	Outside	Inside	Outside	Inside	Outside	Inside	Outside	Inside	Outside	Inside	Outside	Inside	Outside
N	41	32	20	16	21	16	8	6	8	6	8	5	8	5	4	5	5	5
Mean	11.05	7.86	12.13	9.53	10.02	6.19	10.5	10.41	7.13	5.97	12.49	12.49	10.36	7.01	14.69	5.11	14.11	5.62
StDev	5.73	4.44	5.51	4.81	5.88	3.41	6.91	5.16	3.01	3.73	4.83	4.55	4.74	4.57	3.16	0.595	8.95	1.99
SE Mean	0.9	0.78	1.2	1.2	1.3	0.85	2.4	2.1	1.1	1.5	1.7	2	1.7	2	1.6	0.27	4	0.89
C.I.	1.21		-0.31		1.23		-5.7		-2.24		-4.87		-1.56		5.41		-0.25	
t-Calc.	2.69		1.51		2.49		0.03		0.63		0		1.27		5.74		2.07	
t-Crit.	1.671		1.697		1.697		1.796		1.833		1.833		1.86		2.353		2.132	
P-Value	0.005		0.07		0.009		0.488		0.273		0.501		0.12		0.005		0.054	
DF	70		33		32		11		9		9		8		3		4	
Accept/Reject	Accept		Reject		Rejcet		Accept		Accept		Accept		Accept		Reject		Accept	
Alternate Hyp.	Inside-Outside > 0		Inside-Outside > 0		Inside-Outside > 0		Inside-Outside > 0		Inside-Outside > 0		Inside-Outside > 0		Inside-Outside > 0		Inside-Outside > 0		Inside-Outside > 0	

Felsic:
Two Sample T-Test Results

Two-Tail	Bulk		#10		#18		#10 Upper		#18 Upper		#10 Middle		#18 Middle		#10 Lower		#18 Lower	
	Inside	Outside	Inside	Outside	Inside	Outside	Inside	Outside	Inside	Outside	Inside	Outside	Inside	Outside	Inside	Outside	Inside	Outside
N	41	32	20	16	21	16	8	6	8	6	8	5	8	5	4	5	5	5
Mean	18.23	22.63	18.43	19.85	18.05	25.4	18.86	23.46	17.69	30.11	16.26	17.82	16.99	28.18	21.91	17.56	20.3	16.98
StDev	5.01	7.81	5.39	6.53	4.75	8.18	5.94	6.1	5.42	1.95	4.46	4.6	4.8	7.04	5.09	7.81	3.47	8.05
SE Mean	0.78	1.4	1.2	1.6	1	2	2.1	2.5	1.9	0.8	1.6	2.1	1.7	3.2	2.5	3.5	1.6	3.6
C.I.	-7.58, -1.21		-5.58, 2.73		-12.11, -2.61		-11.86, 2.66		-17.11, -7.72		-7.54, 4.42		-19.95, -2.44		-6.23, 14.92		-6.75, 13.40	
t-Calc.	-2.77		-0.7		-3.21		-1.41		-5.98		-0.6		-3.13		1.01		0.85	
t-Crit.	2.009		2.048		2.074		2.228		2.262		2.306		2.447		2.447		2.571	
P-Value	0.008		0.488		0.004		0.188		0		0.564		0.02		0.353		0.435	
DF	50		28		22		10		9		8		6		6		5	
Accept/Reject	Reject		Accept		Reject		Accept		Reject		Accept		Reject		Accept		Accept	
Alternate Hyp.	Inside-Outside ≠ 0		Inside-Outside ≠ 0		Inside-Outside ≠ 0		Inside-Outside ≠ 0		Inside-Outside ≠ 0		Inside-Outside ≠ 0		Inside-Outside ≠ 0		Inside-Outside ≠ 0		Inside-Outside ≠ 0	

One-Tail	Bulk		#10		#18		#10 Upper		#18 Upper		#10 Middle		#18 Middle		#10 Lower		#18 Lower	
	Inside	Outside	Inside	Outside	Inside	Outside	Inside	Outside	Inside	Outside	Inside	Outside	Inside	Outside	Inside	Outside	Inside	Outside
N	41	32	20	16	21	16	8	6	8	6	8	5	8	5	4	5	5	5
Mean	18.23	22.63	18.43	19.85	18.05	25.4	18.86	23.46	17.69	30.11	16.26	17.82	16.99	28.18	21.91	17.56	20.3	16.98
StDev	5.01	7.81	5.39	6.53	4.75	8.18	5.94	6.1	5.42	1.95	4.46	4.6	4.8	7.04	5.09	7.81	3.47	8.05
SE Mean	0.78	1.4	1.2	1.6	1	2	2.1	2.5	1.9	0.8	1.6	2.1	1.7	3.2	2.5	3.5	1.6	3.6
C.I.	1.74		-2.03		3.42		-1.3		8.61		-3.26		4.24		-12.74		-11.22	
t-Calc.	2.77		0.7		3.21		1.41		5.98		0.6		3.13		-1.01		-0.85	
t-Crit.	1.676		1.701		1.717		1.812		1.833		1.86		1.943		1.943		2.015	
P-Value	0.004		0.244		0.002		0.094		0		0.282		0.01		0.823		0.782	
DF	50		28		22		10		9		8		6		6		5	
Accept/Reject	Reject		Accept		Reject		Accept		Reject		Accept		Reject		Accept		Accept	
Alternate Hyp.	Outsie-Inside > 0		Outsie-Inside > 0		Outsie-Inside > 0		Outsie-Inside > 0		Outsie-Inside > 0		Outside-Inside > 0		Outside-Inside > 0		Outside-Inside > 0		Outside-Inside > 0	

Quartzite:
Two Sample T-Test Results

Two-Tail	Bulk		#10		#18		#10 Upper		#18 Upper		#10 Middle		#18 Middle		#10 Lower		#18 Lower	
	Inside	Outside	Inside	Outside	Inside	Outside	Inside	Outside	Inside	Outside	Inside	Outside	Inside	Outside	Inside	Outside	Inside	Outside
N	41	32	20	16	21	16	8	6	8	6	8	5	8	5	4	5	5	5
Mean	13.34	18.71	15.88	22.5	10.92	14.92	18.9	23.51	13.25	15.12	14.82	21.4	10.38	16.58	11.94	22.4	8.06	13.04
StDev	5.99	8.18	5.98	9.04	5.03	5.1	4.25	8.14	4.83	3.31	6.81	5.68	4.97	4.4	5.32	13.7	4.55	7.51
SE Mean	0.94	1.4	1.3	2.3	1.1	1.3	1.5	3.3	1.7	1.4	2.4	2.5	1.8	2	2.7	6.1	2	3.4
C.I.	-8.83, -1.92		-12.05, -1.20		-7.43, -0.58		-13.23, 4.02		-6.66, 2.93		-14.49, 1.34		-12.17, -0.23		-27.66, 6.74		-14.58, 4.64	
t-Calc.	-3.12		-2.52		-2.38		-1.26		-0.86		-1.88		-2.35		-1.56		-1.27	
t-Crit.	2.005		2.064		2.037		2.365		2.201		2.262		2.262		2.571		2.447	
P-Value	0.003		0.019		0.023		0.247		0.41		0.093		0.043		0.179		0.253	
DF	54		24		32		7		11		9		9		5		6	
Accept/Reject	Reject		Reject		Reject		Accept		Accept		Accept		Reject		Accept		Accept	
Alternate Hyp.	Inside-Outside ≠ 0		Inside-Outside ≠ 0		Inside-Outside ≠ 0		Inside-Outside ≠ 0		Inside-Outside ≠ 0		Inside-Outside ≠ 0		Inside-Outside ≠ 0		Inside-Outside ≠ 0		Inside-Outside ≠ 0	

One-Tail	Bulk		#10		#18		#10 Upper		#18 Upper		#10 Middle		#18 Middle		#10 Lower		#18 Lower	
	Inside	Outside	Inside	Outside	Inside	Outside	Inside	Outside	Inside	Outside	Inside	Outside	Inside	Outside	Inside	Outside	Inside	Outside
N	41	32	20	16	21	16	8	6	8	6	8	5	8	5	4	5	5	5
Mean	13.34	18.71	15.88	22.5	10.92	14.92	18.9	23.51	13.25	15.12	14.82	21.4	10.38	16.58	11.94	22.4	8.06	13.04
StDev	5.99	8.18	5.98	9.04	5.03	5.1	4.25	8.14	4.83	3.31	6.81	5.68	4.97	4.4	5.32	13.7	4.55	7.51
SE Mean	0.94	1.4	1.3	2.3	1.1	1.3	1.5	3.3	1.7	1.4	2.4	2.5	1.8	2	2.7	6.1	2	3.4
C.I.	2.49		2.13		1.15		-2.31		-2.05		0.16		1.36		-3.03		-2.66	
t-Calc.	3.12		2.52		2.38		1.26		0.86		1.88		2.35		1.56		1.27	
t-Crit.	1.674		1.711		1.694		1.895		1.796		1.833		1.833		2.015		1.843	
P-Value	0.001		0.009		0.012		0.124		0.205		0.046		0.022		0.089		0.126	
DF	54		24		32		7		11		9		9		5		6	
Accept/Reject	Reject		Reject		Reject		Accept		Acceot		Reject		Reject		Accept		Accept	
Alternate Hyp.	Outsie-Inside > 0		Outsie-Inside > 0		Outsie-Inside > 0		Outsie-Inside > 0		Outsie-Inside > 0		Outside-Inside > 0		Outside-Inside > 0		Outside-Inside > 0		Outside-Inside > 0	

Quartz Grain:
Two Sample T-Test Results

Two-Tail	Bulk		#10		#18		#10 Upper		#18 Upper		#10 Middle		#18 Middle		#10 Lower		#18 Lower	
	Inside	Outside	Inside	Outside	Inside	Outside	Inside	Outside	Inside	Outside	Inside	Outside	Inside	Outside	Inside	Outside	Inside	Outside
N	40	32	20	16	21	16	8	6	8	6	8	5	8	5	4	5	5	5
Mean	10.5	15.38	4.12	9.02	16.17	21.73	3.72	10.41	17.47	22.02	4.35	5.65	17.72	18.21	4.47	10.72	11.59	24.91
StDev	8.27	7.96	2.81	3.68	7.43	5.58	1.98	3.44	7.19	7.35	3.34	1.1	5.56	3.78	3.74	3.75	4.74	2.56
SE Mean	1.3	1.4	0.63	0.92	1.6	1.4	0.7	1.4	2.5	3	1.2	0.49	3	1.7	1.9	1.7	2.1	1.1
C.I.	-8.71, -1.04		-7.18, -2.61		-9.91, -1.22		-10.39, -2.98		-13.31, 4.22		-4.20, 1.60		-8.22, 7.23		-12.40, -0.11		-19.22, -7.43	
t-Calc.	-2.54		-4.4		-2.6		-4.26		-1.16		-1.01		-0.14		-2.49		-5.53	
t-Crit.	1.996		2.052		2.032		2.365		2.228		2.262		2.228		2.447		2.447	
P-Value	0.013		0		0.014		0.004		0.275		0.337		0.889		0.047		0.001	
DF	67		27		34		7		10		9		10		6		6	
Accept/Reject	Reject		Reject		Reject		Reject		Accept		Accept		Accept		Reject		Reject	
Alternate Hyp.	Inside-Outside ≠ 0		Inside-Outside ≠ 0		Inside-Outside ≠ 0		Inside-Outside ≠ 0		Inside-Outside ≠ 0		Inside-Outside ≠ 0		Inside-Outside ≠ 0		Inside-Outside ≠ 0		Inside-Outside ≠ 0	

One-Tail	Bulk		#10		#18		#10 Upper		#18 Upper		#10 Middle		#18 Middle		#10 Lower		#18 Lower	
	Inside	Outside	Inside	Outside	Inside	Outside	Inside	Outside	Inside	Outside	Inside	Outside	Inside	Outside	Inside	Outside	Inside	Outside
N	40	32	20	16	21	16	8	6	8	6	8	5	8	5	4	5	5	5
Mean	10.5	15.38	4.12	9.02	16.17	21.73	3.72	10.41	17.47	22.02	4.35	5.65	17.72	18.21	4.47	10.72	11.59	24.91
StDev	8.27	7.96	2.81	3.68	7.43	5.58	1.98	3.44	7.19	7.35	3.34	1.1	5.56	3.78	3.74	3.75	4.74	2.56
SE Mean	1.3	1.4	0.63	0.92	1.6	1.4	0.7	1.4	2.5	3	1.2	0.49	3	1.7	1.9	1.7	2.1	1.1
C.I.	1.9		4.9		1.95		3.71		-2.58		-1.05		-5.79		1.37		8.64	
t-Calc.	2.66		4.4		2.6		4.26		1.16		1.01		0.14		2.49		5.53	
t-Crit.	1.668		1.703		1.691		1.895		1.812		1.833		1.812		1.943		1.943	
P-Value	0.005		0		0.007		0.002		0.137		0.168		0.445		0.025		0.001	
DF	67		27		34		7		10		9		10		6		6	
Accept/Reject	Reject		Reject		Reject		Reject		Accept		Accept		Accept		Reject		Reject	
Alternate Hyp.	Outsie-Inside > 0		Outsie-Inside > 0		Outsie-Inside > 0		Outsie-Inside > 0		Outsie-Inside > 0		Outside-Inside > 0		Outside-Inside > 0		Outside-Inside > 0		Outside-Inside > 0	

Clastic:
Two Sample T-Test Results

Two-Tail	Bulk		#10		#18		#10 Upper		#18 Upper		#10 Middle		#18 Middle		#10 Lower		#18 Lower	
	Inside	Outside	Inside	Outside	Inside	Outside	Inside	Outside	Inside	Outside	Inside	Outside	Inside	Outside	Inside	Outside	Inside	Outside
N	41	32	20	26	21	16	8	6	8	6	8	5	8	5	4	5	5	5
Mean	11.43	10.44	11.8	11.1	11.08	9.75	8.15	8.46	8.77	7.42	15.25	7.04	12.84	6.22	12.19	18.4	11.96	16.1
StDev	5.59	9.18	6.21	10.1	5.03	8.43	6.12	4.76	6.4	3.01	5.79	4.37	2.89	3.92	3.35	15.4	4.74	12.9
SE Mean	0.87	1.6	1.4	2.5	1.1	2.1	2.2	1.9	2.3	1.2	2	2	1	1.8	1.7	6.9	2.1	5.8
C.I.	-2.71, 4.70		-5.28, 6.65		-3.60, 6.25		-6.70, 6.09		-4.38, 7.09		1.91, 14.51		1.66, 11.59		-25.93, 13.53		-19.90, 11.63	
t-Calc.	0.54		0.24		0.56		-0.11		0.53		2.9		3.26		-0.87		-0.67	
t-Crit.	2.011		2.069		2.074		2.201		2.228		2.228		2.447		2.776		2.571	
P-Value	0.591		0.815		0.582		0.918		0.611		0.016		0.017		0.432		0.53	
DF	48		23		22		11		10		10		6		4		5	
Accept/Reject	Accept		Accept		Accept		Accept		Accept		Reject		Reject		Accept		Accept	
Alternate Hyp.	Inside-Outside ≠ 0		Inside-Outside ≠ 0		Inside-Outside ≠ 0		Inside-Outside ≠ 0		Inside-Outside ≠ 0		Inside-Outside ≠ 0		Inside-Outside ≠ 0		Inside-Outside ≠ 0		Inside-Outside ≠ 0	

One-Tail	Bulk		#10		#18		#10 Upper		#18 Upper		#10 Middle		#18 Middle		#10 Lower		#18 Lower	
	Inside	Outside	Inside	Outside	Inside	Outside	Inside	Outside	Inside	Outside	Inside	Outside	Inside	Outside	Inside	Outside	Inside	Outside
N	41	32	20	16	21	16	8	6	8	6	8	5	8	5	4	5	5	5
Mean	11.43	10.44	11.8	11.1	11.08	9.75	8.15	8.46	8.77	7.42	15.25	7.04	12.84	6.22	12.19	18.4	11.96	16.1
StDev	5.58	9.18	6.21	10.1	5.03	8.43	6.12	4.76	6.4	3.01	5.79	4.37	2.89	3.92	3.35	15.4	4.74	12.9
SE Mean	0.87	1.6	1.4	2.5	1.1	2.1	2.2	1.9	2.3	1.2	2	2	1	1.8	1.7	6.9	2.1	5.8
C.I.	-4.08		-5.62		-5.41		-4.91		-6.02		-13.34		-10.57		-8.95		-8.22	
t-Calc.	-0.54		-0.24		-0.56		0.11		-0.53		-2.9		-3.26		0.87		0.67	
t-Crit.	1.677		1.714		1.717		1.796		1.812		1.812		1.943		2.132		2.015	
P-Value	0.704		0.592		0.709		0.459		0.695		0.992		0.991		0.216		0.265	
DF	48		23		22		11		10		10		6		4		5	
Accept/Reject	Accept		Accept		Accept		Accept		Accept		Accept		Accept		Accept		Accept	
Alternate Hyp.	Outsie-Inside > 0		Outsie-Inside > 0		Outsie-Inside > 0		Outsie-Inside > 0		Outsie-Inside > 0		Outside-Inside > 0		Outside-Inside > 0		Outside-Inside > 0		Outside-Inside > 0	

Limestone/Dolomite:
Two Sample T-Test Results

Two-Tail	Bulk		#10		#18		#10 Upper		#18 Upper		#10 Middle		#18 Middle		#10 Lower		#18 Lower	
	Inside	Outside	Inside	Outside	Inside	Outside	Inside	Outside	Inside	Outside	Inside	Outside	Inside	Outside	Inside	Outside	Inside	Outside
N	41	32	20	16	21	16	8	6	8	6	8	5	8	5	4	5	5	5
Mean	25.64	21.6	30.28	24.3	21.21	18.8	32.2	19.5	25.5	15.1	29.11	31.73	18.49	21.401	28.84	22.65	18.73	20.64
StDev	9.45	10.1	8.09	11.2	8.62	8.29	10.8	16.2	10.3	12.2	6.51	3.25	6.77	0.571	5.35	4.73	6.88	6.28
SE Mean	1.5	1.8	1.8	2.8	1.9	2.1	3.8	6.6	3.6	5	2.3	1.5	2.4	0.26	2.7	2.1	3.1	2.8
C.I.	-0.54, 8.70		-0.87, 12.81		-3.28, 8.10		-4.93, 30.27		-3.52, 24.29		-8.68, 3.45		-8.61, 2.78		-2.15, 14.52		-11.75, 7.95	
t-Calc.	1.77		1.8		0.86		1.66		1.69		-0.96		-1.21		1.82		-0.46	
t-Crit.	1.998		2.056		2.035		2.306		2.262		2.228		2.365		2.447		2.365	
P-Value	0.082		0.084		0.395		0.136		0.126		0.359		0.266		0.119		0.661	
DF	64		26		33		8		9		10		7		6		7	
Accept/Reject	Accept		Accept		Accept		Accept		Accept		Accept		Accept		Accept		Accept	
Alternate Hyp.	Inside-Outside ≠ 0		Inside-Outside ≠ 0		Inside-Outside ≠ 0		Inside-Outside ≠ 0		Inside-Outside ≠ 0		Inside-Outside ≠ 0		Inside-Outside ≠ 0		Inside-Outside ≠ 0		Inside-Outside ≠ 0	

One-Tail	Bulk		#10		#18		#10 Upper		#18 Upper		#10 Middle		#18 Middle		#10 Lower		#18 Lower	
	Inside	Outside	Inside	Outside	Inside	Outside	Inside	Outside	Inside	Outside	Inside	Outside	Inside	Outside	Inside	Outside	Inside	Outside
N	41	32	20	16	21	16	8	6	8	6	8	5	8	5	4	5	5	5
Mean	25.64	21.6	30.28	24.3	21.21	18.8	32.2	19.5	25.5	15.1	29.11	31.73	18.49	21.401	28.84	22.65	18.73	20.64
StDev	9.45	10.1	8.09	11.2	8.62	8.29	10.8	16.2	10.3	12.2	6.51	3.25	6.77	0.571	5.35	4.73	6.88	6.28
SE Mean	1.5	1.8	1.8	2.8	1.9	2.1	3.8	6.6	3.6	5	2.3	1.5	2.4	0.26	2.7	2.1	3.1	2.8
C.I.	0.22		0.3		-2.32		-1.53		-0.89		-7.55		-7.48		-0.43		-9.8	
t-Calc.	1.77		1.8		0.86		1.66		1.69		-0.96		-1.21		1.82		-0.46	
t-Crit.	1.669		1.706		1.692		1.86		1.833		1.812		1.895		1.943		1.895	
P-Value	0.041		0.042		0.197		0.068		0.063		0.82		0.867		0.06		0.669	
DF	64		26		33		8		9		10		7		6		7	
Accept/Reject	Reject		Reject		Accept		Accept		Accept		Accept		Accept		Accept		Accept	
Alternate Hyp.	Inside-Outside > 0		Inside-Outside > 1		Inside-Outside > 2		Inside-Outside > 3		Inside-Outside > 4		Inside-Outside > 5		Inside-Outside > 6		Inside-Outside > 7		Inside-Outside > 8	

Appendix B
Sand Grain Lithology Data

Sample: CA-14-12 (0-5)				
Lithology	**Sieve #10**		**Sieve #18**	
	Number	**Percentage**	**Number**	**Percentage**
Shale	8	8	8	8
Mafic	19	19	12	12
Felsic	26	26	30	29
Quartzite	29	29	15	15
Quartz Grain	13	13	30	29
Clastic	5	5	7	7
Limestone/Dolomite	0	0	0	0
Total	**100**	**100**	**102**	**100**

Sample: CA-14-12 (5-10)				
Lithology	**Sieve #10**		**Sieve #18**	
	Number	**Percentage**	**Number**	**Percentage**
Shale	4	3	0	0
Mafic	6	5	6	6
Felsic	20	17	29	29
Quartzite	22	19	17	17
Quartz Grain	9	8	19	19
Clastic	20	17	7	7
Limestone/Dolomite	37	31	21	21
Total	**118**	**100**	**99**	**100**

Sample: CA-14-12 (10-15)				
Lithology	**Sieve #10**		**Sieve #18**	
	Number	**Percentage**	**Number**	**Percentage**
Shale	2	2	0	0
Mafic	9	9	3	3
Felsic	25	25	28	28
Quartzite	31	31	17	17
Quartz Grain	5	5	28	28
Clastic	4	4	3	3
Limestone/Dolomite	24	24	20	20
Total	**100**	**100**	**99**	**100**

Sample: CA-14-12 (20-25)				
Lithology	**Sieve #10**		**Sieve #18**	
	Number	**Percentage**	**Number**	**Percentage**
Shale	2	2	2	2
Mafic	19	16	3	3
Felsic	20	17	27	27
Quartzite	23	19	17	17
Quartz Grain	8	7	21	21
Clastic	12	10	9	9
Limestone/Dolomite	34	29	21	21
Total	**118**	**100**	**100**	**100**

Sample: CA-14-12 (25-30)				
Lithology	**Sieve #10**		**Sieve #18**	
	Number	**Percentage**	**Number**	**Percentage**
Shale	3	3	1	1
Mafic	11	11	13	13
Felsic	18	18	22	22
Quartzite	15	15	10	10
Quartz Grain	6	6	22	22
Clastic	11	11	10	10
Limestone/Dolomite	36	36	22	22
Total	**100**	**100**	**100**	**101**

Sample: CA-14-12 (40-45)				
Lithology	**Sieve #10**		**Sieve #18**	
	Number	**Percentage**	**Number**	**Percentage**
Shale	3	3	4	4
Mafic	6	6	5	5
Felsic	26	24	28	28
Quartzite	31	29	22	22
Quartz Grain	10	9	23	23
Clastic	6	6	5	5
Limestone/Dolomite	26	24	13	13
Total	**108**	**100**	**100**	**100**

Sample: CA-14-12 (45-50)				
Lithology	**Sieve #10**		**Sieve #18**	
	Number	**Percentage**	**Number**	**Percentage**
Shale	2	2	4	4
Mafic	6	5	10	9
Felsic	26	24	12	11
Quartzite	35	32	20	18
Quartz Grain	10	9	27	25
Clastic	9	8	6	5
Limestone/Dolomite	22	20	31	28
Total	**110**	**100**	**110**	**100**

Sample: CA-14-12 (50-55)				
Lithology	**Sieve #10**		**Sieve #18**	
	Number	**Percentage**	**Number**	**Percentage**
Shale	1	1	2	2
Mafic	6	6	5	5
Felsic	22	22	23	23
Quartzite	36	36	14	14
Quartz Grain	11	11	28	28
Clastic	8	8	10	10
Limestone/Dolomite	16	16	18	18
Total	**100**	**100**	**100**	**100**

Sample: CA-14-16 (0-5 A (1))				
Lithology	**Sieve #10**		**Sieve #18**	
	Number	**Percentage**	**Number**	**Percentage**
Shale	2	2	6	6
Mafic	6	6	1	1
Felsic	19	19	35	34
Quartzite	10	10	9	9
Quartz Grain	14	14	20	19
Clastic	10	10	12	12
Limestone/Dolomite	39	39	21	20
Total	**100**	**100**	**104**	**100**

Sample: CA-14-16 (5-8.5 A)				
Lithology	**Sieve #10**		**Sieve #18**	
	Number	**Percentage**	**Number**	**Percentage**
Shale	6	6	11	11
Mafic	10	10	7	7
Felsic	34	34	29	29
Quartzite	30	30	17	17
Quartz Grain	12	12	26	26
Clastic	9	9	10	10
Limestone/Dolomite	0	0	0	0
Total	**101**	**100**	**100**	**100**

Sample: CA-14-16 (8.5-18.5 B)				
Lithology	**Sieve #10**		**Sieve #18**	
	Number	**Percentage**	**Number**	**Percentage**
Shale	5	4	1	1
Mafic	16	13	7	7
Felsic	24	20	31	31
Quartzite	27	23	16	16
Quartz Grain	13	11	10	10
Clastic	7	6	6	6
Limestone/Dolomite	27	23	29	29
Total	**119**	**100**	**100**	**100**

Sample: CA-14-16 (18.5-28.5 B)				
Lithology	**Sieve #10**		**Sieve #18**	
	Number	**Percentage**	**Number**	**Percentage**
Shale	4	4	4	4
Mafic	7	7	2	2
Felsic	25	25	39	39
Quartzite	18	18	15	15
Quartz Grain	4	4	13	13
Clastic	9	9	6	6
Limestone/Dolomite	32	32	21	21
Total	**99**	**100**	**100**	**100**

Sample: CA-14-16 (28.5-38.5 C)				
Lithology	**Sieve #10**		**Sieve #18**	
	Number	**Percentage**	**Number**	**Percentage**
Shale	5	5	2	2
Mafic	20	18	8	8
Felsic	14	13	31	31
Quartzite	32	29	22	22
Quartz Grain	7	6	16	16
Clastic	1	1	0	0
Limestone/Dolomite	31	28	22	22
Total	**110**	**100**	**101**	**100**

Sample: CA-14-16 (38.5-48.5 C)				
Lithology	**Sieve #10**		**Sieve #18**	
	Number	**Percentage**	**Number**	**Percentage**
Shale	6	6	4	4
Mafic	10	10	9	9
Felsic	16	16	22	22
Quartzite	25	25	19	19
Quartz Grain	5	5	19	19
Clastic	4	4	6	6
Limestone/Dolomite	33	33	21	21
Total	**99**	**100**	**100**	**100**

Sample: CA-14-16 (118.5-128.5 A)				
Lithology	**Sieve #10**		**Sieve #18**	
	Number	**Percentage**	**Number**	**Percentage**
Shale	1	1	1	1
Mafic	6	6	5	5
Felsic	9	9	13	13
Quartzite	10	10	4	4
Quartz Grain	17	17	22	22
Clastic	32	32	29	29
Limestone/Dolomite	25	25	26	26
Total	**100**	**100**	**100**	**100**

Sample: CA-14-16 (118.5-128.5 B)				
Lithology	**Sieve #10**		**Sieve #18**	
	Number	**Percentage**	**Number**	**Percentage**
Shale	8	7	3	3
Mafic	5	5	4	4
Felsic	10	9	10	10
Quartzite	6	5	7	7
Quartz Grain	8	7	27	27
Clastic	42	38	31	31
Limestone/Dolomite	31	28	18	18
Total	**110**	**100**	**100**	**100**

Sample: CA-14-10 (0-5 (4))				
Lithology	**Sieve #10**		**Sieve #18**	
	Number	**Percentage**	**Number**	**Percentage**
Shale	8	8	13	6
Mafic	3	3	9	4
Felsic	15	16	28	13
Quartzite	19	20	43	20
Quartz Grain	6	6	61	29
Clastic	2	2	5	2
Limestone/Dolomite	43	45	54	25
Total	**96**	**100**	**213**	**100**

Sample: CA-14-10 (10-15 (2))				
Lithology	**Sieve #10**		**Sieve #18**	
	Number	**Percentage**	**Number**	**Percentage**
Shale	7	7	9	7
Mafic	10	9	9	7
Felsic	12	11	13	10
Quartzite	13	12	15	11
Quartz Grain	5	5	33	25
Clastic	8	7	3	2
Limestone/Dolomite	52	49	51	38
Total	**107**	**100**	**133**	**100**

Sample: CA-14-10 (15-20 (2))				
Lithology	**Sieve #10**		**Sieve #18**	
	Number	**Percentage**	**Number**	**Percentage**
Shale	9	9	13	12
Mafic	1	1	4	4
Felsic	29	29	22	20
Quartzite	23	23	10	9
Quartz Grain	3	3	13	12
Clastic	2	2	4	4
Limestone/Dolomite	34	34	44	40
Total	**101**	**100**	**110**	**100**

Sample: CA-14-10 (15-20 (5))				
Lithology	**Sieve #10**		**Sieve #18**	
	Number	**Percentage**	**Number**	**Percentage**
Shale	9	9	10	10
Mafic	8	8	6	6
Felsic	17	17	12	12
Quartzite	24	24	18	18
Quartz Grain	4	4	19	19
Clastic	2	2	4	4
Limestone/Dolomite	36	36	32	32
Total	**100**	**100**	**101**	**100**

Sample: CA-14-10 (20-25 (1))				
Lithology	**Sieve #10**		**Sieve #18**	
	Number	**Percentage**	**Number**	**Percentage**
Shale	9	10	8	8
Mafic	2	2	4	4
Felsic	16	18	20	19
Quartzite	25	29	20	19
Quartz Grain	1	1	21	20
Clastic	7	8	10	9
Limestone/Dolomite	27	31	23	22
Total	**87**	**100**	**106**	**100**

Sample: CA-14-10 (35-40 (2))				
Lithology	**Sieve #10**		**Sieve #18**	
	Number	**Percentage**	**Number**	**Percentage**
Shale	5	5	13	13
Mafic	12	12	19	19
Felsic	15	15	21	21
Quartzite	17	17	4	4
Quartz Grain	10	10	15	15
Clastic	9	9	13	13
Limestone/Dolomite	33	33	16	16
Total	**101**	**100**	**101**	**100**

Sample: CA-14-10 (40-45 (2))				
Lithology	**Sieve #10**		**Sieve #18**	
	Number	**Percentage**	**Number**	**Percentage**
Shale	5	5	6	6
Mafic	15	15	11	11
Felsic	21	21	20	20
Quartzite	8	8	8	8
Quartz Grain	9	9	20	20
Clastic	17	17	16	16
Limestone/Dolomite	25	25	19	19
Total	**100**	**100**	**100**	**100**

Sample: CA-14-10 (65-67.5 (2))				
Lithology	**Sieve #10**		**Sieve #18**	
	Number	**Percentage**	**Number**	**Percentage**
Shale	6	6	9	9
Mafic	8	8	12	12
Felsic	18	18	11	11
Quartzite	18	18	25	25
Quartz Grain	10	10	22	22
Clastic	12	12	6	6
Limestone/Dolomite	28	28	15	15
Total	**100**	**100**	**100**	**100**

Sample: CA-15-05 (10-15)				
Lithology	**Sieve #10**		**Sieve #18**	
	Number	**Percentage**	**Number**	**Percentage**
Shale	6	6	3	3
Mafic	20	20	10	9
Felsic	22	22	26	24
Quartzite	18	18	20	18
Quartz Grain	4	4	16	15
Clastic	11	11	14	13
Limestone/Dolomite	19	19	20	18
Total	**100**	**100**	**109**	**100**

Sample: CA-15-05 (15-20)				
Lithology	**Sieve #10**		**Sieve #18**	
	Number	**Percentage**	**Number**	**Percentage**
Shale	11	11	13	13
Mafic	13	13	11	11
Felsic	26	25	22	22
Quartzite	17	17	9	9
Quartz Grain	6	6	20	20
Clastic	8	8	12	12
Limestone/Dolomite	21	21	14	14
Total	**102**	**100**	**101**	**100**

Sample: CA-15-05 (20-25)				
Lithology	**Sieve #10**		**Sieve #18**	
	Number	**Percentage**	**Number**	**Percentage**
Shale	10	10	18	17
Mafic	19	19	9	8
Felsic	14	14	11	10
Quartzite	18	18	6	6
Quartz Grain	1	1	39	37
Clastic	14	14	18	17
Limestone/Dolomite	26	25	5	5
Total	**102**	**100**	**106**	**100**

Sample: CA-15-05 (25-30)				
Lithology	**Sieve #10**		**Sieve #18**	
	Number	**Percentage**	**Number**	**Percentage**
Shale	4	4	18	16
Mafic	14	13	8	7
Felsic	13	12	11	10
Quartzite	8	8	17	15
Quartz Grain	4	4	19	17
Clastic	28	27	11	10
Limestone/Dolomite	34	32	30	26
Total	**105**	**100**	**114**	**100**

Sample: CA-15-05 (30-35)				
Lithology	**Sieve #10**		**Sieve #18**	
	Number	**Percentage**	**Number**	**Percentage**
Shale	12	12	14	14
Mafic	14	14	8	8
Felsic	20	20	23	23
Quartzite	16	16	8	8
Quartz Grain	4	4	11	11
Clastic	15	15	15	15
Limestone/Dolomite	19	19	21	21
Total	**100**	**100**	**100**	**100**

Sample: CA-15-05 (35-40)				
Lithology	**Sieve #10**		**Sieve #18**	
	Number	**Percentage**	**Number**	**Percentage**
Shale	5	5	4	4
Mafic	19	19	25	23
Felsic	23	23	21	19
Quartzite	16	16	13	12
Quartz Grain	4	4	15	14
Clastic	12	12	14	13
Limestone/Dolomite	21	21	18	16
Total	**100**	**100**	**110**	**100**

Sample: CA-15-05 (45-50)				
Lithology	**Sieve #10**		**Sieve #18**	
	Number	**Percentage**	**Number**	**Percentage**
Shale	9	9	14	13
Mafic	15	15	22	20
Felsic	27	27	26	24
Quartzite	6	6	5	5
Quartz Grain	2	2	17	15
Clastic	11	11	9	8
Limestone/Dolomite	30	30	17	15
Total	**100**	**100**	**110**	**100**

Sample: CA-15-05 Average				
Lithology	**Sieve #10**		**Sieve #18**	
	Number	**Percentage**	**Number**	**Percentage**
Shale	8	8	12	11
Mafic	16	16	13	12
Felsic	21	21	20	19
Quartzite	14	14	11	10
Quartz Grain	4	4	20	18
Clastic	14	14	13	12
Limestone/Dolomite	24	24	18	17
Total	**101**	**100**	**107**	**100**

Sample: CA-15-08 (5-10)				
Lithology	**Sieve #10**		**Sieve #18**	
	Number	**Percentage**	**Number**	**Percentage**
Shale	6	6	14	13
Mafic	20	20	12	11
Felsic	16	16	19	18
Quartzite	15	15	13	12
Quartz Grain	1	1	16	15
Clastic	18	18	16	15
Limestone/Dolomite	25	25	15	14
Total	**101**	**100**	**105**	**100**

Sample: CA-15-08 (10-15)				
Lithology	**Sieve #10**		**Sieve #18**	
	Number	**Percentage**	**Number**	**Percentage**
Shale	6	6	18	18
Mafic	10	10	5	5
Felsic	15	15	23	23
Quartzite	23	23	8	8
Quartz Grain	1	1	6	6
Clastic	15	15	18	18
Limestone/Dolomite	30	30	22	22
Total	**100**	**100**	**100**	**100**

Sample: CA-15-08 (25-30)				
Lithology	**Sieve #10**		**Sieve #18**	
	Number	**Percentage**	**Number**	**Percentage**
Shale	9	9	20	20
Mafic	10	10	15	15
Felsic	21	21	17	17
Quartzite	13	13	11	11
Quartz Grain	3	3	10	10
Clastic	18	18	12	12
Limestone/Dolomite	27	27	15	15
Total	**101**	**100**	**100**	**100**

Sample: CA-15-08 (30-35)				
Lithology	**Sieve #10**		**Sieve #18**	
	Number	**Percentage**	**Number**	**Percentage**
Shale	7	7	14	13
Mafic	15	15	12	11
Felsic	9	9	18	16
Quartzite	11	11	14	13
Quartz Grain	3	3	14	13
Clastic	15	15	12	11
Limestone/Dolomite	41	41	27	24
Total	**101**	**100**	**111**	**100**

Sample: CA-15-08 (40-45)				
Lithology	**Sieve #10**		**Sieve #18**	
	Number	**Percentage**	**Number**	**Percentage**
Shale	0	0	34	34
Mafic	0	0	3	3
Felsic	0	0	23	23
Quartzite	0	0	14	14
Quartz Grain	0	0	4	4
Clastic	0	0	7	7
Limestone/Dolomite	0	0	15	15
Total	**0**	**0**	**100**	**100**

Sample: CA-15-08 (45-50)				
Lithology	**Sieve #10**		**Sieve #18**	
	Number	**Percentage**	**Number**	**Percentage**
Shale	5	5	13	13
Mafic	13	13	6	6
Felsic	23	23	15	15
Quartzite	9	9	6	6
Quartz Grain	2	2	10	10
Clastic	17	17	19	19
Limestone/Dolomite	32	32	31	31
Total	**101**	**100**	**100**	**100**

BIBLIOGRAPHY

Anderson, R.C., 1957. Pebble and sand lithology of the major Wisconsin glacial lobes of the Central Lowland, Bulletin of the Geological Society of America 68, 1415-1450

Barnes, N. A., 2007. Stratigraphy and Organic Carbon Contents of Glacial Deposits in the City of Portage, Michigan, U.S.A., M.S. Thesis, Western Michigan University, Kalamazoo, 188 p.

Bedrock Geology of Michigan, 1987. Michigan Department of Environmental Quality (MDEQ) - Geologic Survey Division. Lansing, MI, MDEQ.

Benn, D.I., and Evans, D.J., 2010. Glaciers & Glaciation, 2nd edition, Hodder Education, London U.K., 802 pp.

Beukema, S. P., 2003. Stratigraphy of Lake Michigan lobe deposits in Van Buren County Michigan. M.S. Thesis, Western Michigan University, Kalamazoo. 140 p.

Bowles, 1978. Engineering Properties of Soils and their Measurement (2nd edition): McGraw-Hill, New York, 213 pp.

Curry, B., Petras, J., 2011. Chronological framework for the deglaciation of the Lake Michigan lobe of the Laurentide Ice Sheet from ice-walled lake deposits. Journal of Quaternary Science. 26, 402-410.

Curry, B. B., Hajic, E. R., Clark, J. A., Befus, K. M., Carrell, J. E., & Brown, S. E. 2014. The Kankakee Torrent and Other Large Meltwater Flooding Events during the Last Deglaciation, Illinois, USA. Quaternary Science Reviews, 90, 22-36.

Dodson, R. L., 1985. Topographic and sedimentary characteristics of the Union Streamlined Plain and surrounding areas. Ph.D. dissertation, Michigan State University, East Lansing, 169 p.

Dorr, J.A., Eschman D.F., 1970. Geology of Michigan. The University of Michigan Press, Ann Arbor, 476 p.

Ewald, S. K., 2012. Stratigraphic Framework for Deposits of the Saginaw lobe, Barry and Calhoun Counties, Michigan, USA. M.S. Thesis. Western Michigan University, 295 p.

Eyles, Nick, 2012. "Rock Drumlins and Megaflutes of the Niagara Escarpment, Ontario, Canada; a Hard Bed Landform Assemblage Cut by the Saginaw-Huron Ice Stream." Quaternary Science Reviews 55: 34-49.

Farrand, W. R., Bell, D.L., 1982. Quaternary geology of southern Michigan: Lansing, MI, Michigan Department of Natural Resources.

Fisher, T.G., and Jol, H.M., Taylor, L., D., 2005. Saginaw Lobe tunnel channels (Laurentide Ice Sheet) and their significance in south-central Michigan, USA, Quaternary Science Reviews 24: 2375–2391.

Fisher, T.G., and Taylor, L., D., 1999, Glacial landforms and sediment landform assemblages, Saginaw Lobe, in Brown, S.E., Fisher, T.G., Kehew, A.E., and Taylor, L., D., eds., Guidebook for the 45th Midwest Friends of the 131 Pleistocene Field Conference: Bloomington, IN, Indiana Geological Survey, p. 82.

Fisher, T.G., Taylor, L., D., and Jol, H.M., 2003. Boulder-gravel hummocks and wavy basal till contacts: Products of subglacial meltwater flow beneath the Saginaw Lobe, south-central Michigan, USA: Boreas, 32: 328-336.

Fisher, T.G., and Taylor, L., D., 2002. Sedimentary and stratigraphic evidence for subglacial flooding, south-central Michigan, USA, Quaternary International 90: 87-115.

Flint, A. C., 1999. Stratigraphic Analysis of Diamicton units in North-Central St. Joseph County, Michigan. M.S. Thesis, Western Michigan University, Kalamazoo.

Gillespie, R., Harrison III, W. B., and Grammer, G. M., 2008. Geology of Michigan and the Great Lakes. Michigan Geological Repository for Research and Education, Western Michigan University, 37 p.

Hobbs, Howard C., 1998. "Use of 1-2-Millimeter Sand-Grain Composition in Minnesota Quaternary Studies." Report of Investigations - Minnesota Geological Survey: 193-208.

Howard, J. L., Coram, M. and Zawiskie, J. M., 2012, Stratigraphy, paleoenvironments and provenance of gravelly glacial sediments, southeastern Michigan: Implications for late Pleistocene paleogeography and ice-flow movements, In: Muller, J., and Koch, L. (eds.), Ice sheets: Dynamics, formation and environmental concerns, Nova Pub., New York, p.1-54.

Johnson, W.H., Hansel, A.K., Bettis, E.A., III, Karrow, P.F., Larson, G.J., Lowell, T.V., and Schneider, A.F., 1997. Late Quaternary temporal and event classifications, Great Lakes region, North America. Quaternary Research 47: 1-12.

Karrow, Paul F., Aleksis Dreimanis, and Peter J. Barnett., 2000. "A Proposed Diachronic Revision of Late Quaternary Time-Stratigraphic Classification in the Eastern and Northern Great Lakes Area." Quaternary Research 54.1: 1-12.

Kehew, A.E., Nicks, L.P. and Straw, T.W., 1999. Palimpsest tunnel valleys: evidence for relative timing of advances in an interlobate area of the Laurentide ice sheet, Annals of Glaciology 28, pp. 47–52.

Kehew, A.E., Beukema, P.S., Brian, C. B., and Kozlowski, A. L., 2005. Fast flow of the Lake Michigan lobe: evidence from sediment-landform assemblages in southwestern Michigan, U.S.A. Quaternary Science Reviews 24: 2335-2353.

Kehew, A. E., Esch J. M., Kozlowski, A. L., Ewald, S. K., 2012a. Glacial landsystems and dynamics of the Saginaw lobe of the Laurentide Ice Sheet, Michigan, USA, Quaternary International 260: 21-31.

Kehew, A.E., Piotrowski, J.A., Jorgensen, F., 2012b. Tunnel Valleys: Concepts and controversies-A review, Earth-Science Reviews 113: 33-58.

Kozlowski, A.L., 1999. Three dimensional mapping of the East Leroy and Union City 7.5 minute quadrangles in southwest Michigan. M.S. Thesis, Western Michigan University, Kalamazoo.

Kozlowski, A.L., Kehew, A.E., and Bird, B.C., 2001. An outburst hypothesis for the origin of the Kalamazoo river valley, Kalamazoo and Allegan counties. Michigan, Geological Society of America Abstracts with Programs 33 (7), p. 269.

Kozlowski, A.L., 2004. Origin of the Central Kalamazoo River Valley, Southwestern Michigan, USA. Ph.D. Dissertation, Western Michigan University, Kalamazoo.

Kozlowski, A.L., Kehew, A.E., and Bird, B.C., 2005. Outburst flood origin of the Central Kalamazoo River Valley, Michigan, USA. Quaternary Science Reviews 24: 2354-2374.

Larson, G. L., & Kincare, K., 2009. Late Quaternary History of the Eastern Mid-Continent Region, USA. In: Schaetzl, R (ed), Michgian Geography and Geology Pearson, New York.

Leverett, F., Taylor, F.B., 1915. The Pleistocene of Indiana and Michigan and the history of the Great lakes. United States Geological Survey Monograph 53.

LoDuca, S., 2009. Late Quaternary History of the Eastern Mid-Continent Region, USA. In: Schaetzl, R (ed), Michgian Geography and Geology Pearson, New York.

Lovan, N. A., 1977. Analysis of an Interlobate Boundary in the Wisconsinan Drift of kalamazoo county and Adjacent Areas in Southwestern Michigan. M.S. Thesis, Western Michigan University, 129 p.

Martin, H. M., comp., 1955. Map of the surface formation of the southern Peninsula of Michigan. Michigan Geological Survey, Publication 49.

Monaghan, G.W., and Larson, G.J., 1986. Late Wisconsinan drift stratigraphy of the Saginaw Ice Lobe in south-central Michigan. Geological Society of America Bulletin 97: 324–328.

Nicks, L., 2004. The glacial geology of southern St. Joseph County, Michigan. Ph.D. Dissertation, Western Michigan University, Kalamazoo.

Ohio Division of Geological Survey, 2006, Bedrock geologic map of Ohio: Ohio Department of Natural Resources, Division of Geological Survey Map BG-1

Rieck, R.L., and Winters, H.A., 1982. Characteristics of a Glacially Buried Cuesta in Southeast Michigan. Annals of the Association of American Geographers 72, 482-494

Shah, B.P., 1971. Evaluation of Natural Aggregates in Kalamazoo County and Vicinity, Michigan. Ph. D. Dissertation, Michigan State University, East Lansing, 192 pp.

Taylor, L.D., Fisher, T.G., Jol, H.M. and Okraszewski, M.A., 1998, Stratigraphic evidence for a late Pleistocene glacial outburst flood sequence in south-central Michigan. Geological Society of America, North-central section, Program with abstracts, v. 32, 74.

Woolever, C. J., 2008. Origin of Esker and Tunnel Valley Assemblages in the Saginaw lobe, Barry County, Michigan. M.S. Thesis, Western Michigan University, Kalamazoo, 132 pp.